

8-2012

Preparation of Copper-Based Oxygen Carrier Supported on Titanium Dioxide

Yaowen Cui

Western Kentucky University, yaowen.cui897@topper.wku.edu

Follow this and additional works at: <http://digitalcommons.wku.edu/theses>



Part of the [Environmental Chemistry Commons](#)

Recommended Citation

Cui, Yaowen, "Preparation of Copper-Based Oxygen Carrier Supported on Titanium Dioxide" (2012). *Masters Theses & Specialist Projects*. Paper 1192.

<http://digitalcommons.wku.edu/theses/1192>

This Thesis is brought to you for free and open access by TopSCHOLAR®. It has been accepted for inclusion in Masters Theses & Specialist Projects by an authorized administrator of TopSCHOLAR®. For more information, please contact topscholar@wku.edu.

PREPARATION OF COPPER-BASED OXYGEN CARRIER SUPPORTED ON
TITANIUM DIOXIDE

A Thesis
Presented to
The Faculty of the Department of Chemistry
Western Kentucky University
Bowling Green, Kentucky

In Partial Fulfillment
Of the Requirements for the Degree
Master of Science

By
Yaowen Cui

August 2012

PREPARATION OF COPPER-BASED OXYGEN CARRIER SUPPORTED ON
TITANIUM DIOXIDE

Date Recommended August 8 2012

Wei-ping Pan

Dr. Wei-Ping Pan, Director of Thesis

Yan Cao

Dr. Yan Cao, Director of Thesis

Bangbo Yan

Dr. Bangbo Yan

Rui Zhang

Dr. Rui Zhang

[Signature] 8/27/12
Dean, Graduate Studies and Research Date

ACKNOWLEDGEMENTS

First and foremost I want to thank my advisor, Dr. Wei-Ping Pan, Director of the Institute for Combustion Science and Environmental Technology (ICSET) for providing the opportunity to work on this interesting and meaningful project. He taught me to organize my time and efficiently plan my tasks. He taught me not to be afraid of failing. As a research scientist, some failure is inevitable, but the failure provides learning and improvement opportunities. I am thankful for the excellent example he has provided as a successful scientist and professor.

I would like to thank Dr. Yan Cao for his smart and creative ideas, which are always unique and productive. He always finds the root cause of a problem. He has the ability to put a confusing theory or phenomenon into an easy model to explain. His attitude towards research inspires me with confidence and interest. “Can do” is a phrase we usually hear from him. No difficulty can stop him from doing his research. He sets a very good example for me to follow. During my two years here, his action and instructions have taught me how to be a better student and scientist.

I would like to express my appreciation to Dr. Hou-Yin Zhao. She gave me the benefit of her research experience and I learned a great deal. She has studied oxygen carriers for more than three years. Her sample characterization and activity test experience saved me a lot of time.

I am grateful for Dr. Quentin Lineberry’s great help on thermal analysis operation. He is an expert on TGA, SDT, and DSC operation and repair. Every time I had a problem with an instrument, he was always the man I came to. Also, he taught me how to use the XRD, which I used almost every week in the last year.

I would also like to thank my friend in ICSET. Kelin Wang is a trustful and kind-hearted friend. She always took her time to help me. I am grateful to have a classmate and co-worker like her. William Orndorff, Martin Cohron, Kevin Duckett, Terrill Martin, Lois Hall, and all the exchange students are thanked for their care and attention.

Last but not least, I am fully indebted to the endless encouragement from my parents, grandma and my girlfriend. It is them who support me on my spirit world and give me the power to overcome the hard times and kept me moving forward.

All of that I will always remember.

TABLE OF CONTENTS

1. Introduction.....	1
1.1 Objective.....	1
1.2 Chemical-Looping Combustion (CLC).....	1
1.3 Oxygen Carrier.....	8
1.4 Preparation Methods.....	14
2. Experimental.....	16
2.1 Preparation of Oxygen Carrier.....	16
2.2 Characterization.....	22
2.3 Performance Tests.....	24
2.4 Data Reduction Mathematics.....	27
2.5 Kinetics.....	28
3. Result and Discussion.....	30
3.1 Preparation Factors.....	30
3.2 Titanium(IV) Dioxide Versus Alumina Supporting.....	40
3.3 Activity Test.....	42
4. Conclusion.....	54
5. Future Work.....	56
BIBLIOGRAPHY:.....	57
ACTIVITIES.....	61
Presentation:.....	61
Publication:.....	61

LIST OF FIGURES

Figure 1. Surface temperature change of the earth from 1880 to 2010.	2
Figure 2. Atmospheric CO ₂ concentrations in the air.	3
Figure 3. The layout of green coal combustion process.	4
Figure 4. Gasification carbon dioxide capture process.	5
Figure 5. Oxy-firing carbon dioxide capture process.	6
Figure 6. The theory of chemical-looping combustion.....	7
Figure 7. Variation of the thermodynamic equilibrium factor for Me _x O _y -CO as a function of temperature.	13
Figure 8. Process of mechanical mixing preparation method.....	16
Figure 9. Ball mill.	17
Figure 10. Process of wet-impregnation preparation method.....	18
Figure 11. The process of co-precipitation preparation method.	19
Figure 12. Process of sol-gel preparation method.	20
Figure 13. Across International KTL 1400 Tube Furnace.....	22
Figure 14. Thermo ARL powder X-Ray Diffraction.	23
Figure 15. The X-Ray beam and detector of XRD.	23
Figure 16. JSM-5400LV Scanning Electron Microscope.....	24
Figure 17. TGA and gas auto-switcher system.....	26
Figure 18. Schematic drawing of the thermogravimetric analyzer.....	27
Figure 19. TGA plot of precursor of the sample calcination.	30
Figure 20. XRD pattern of oxygen carrier calcinated from different temperature.	31
Figure 21. Oxygen carrier calcinated at 650°C.....	32

Figure 22. Oxygen carrier calcinated at 800°C.....	33
Figure 23. Oxygen carrier calcinated at 1350°C.....	33
Figure 24. SEM picture of prepared titanium(IV) oxide.	34
Figure 25. Dispersion of oxygen carrier prepared from different method.....	37
Figure 26. Oxygen carrier calcinated at 800°C.....	38
Figure 27. Alumina as an oxygen carrier support at 650°C (solid line) and 800°C (dashed line).	40
Figure 28. Titanium(IV) oxide as an oxygen carrier support at 650°C and 800°C.	41
Figure 29. XRD pattern of oxygen carriers before, after cycles and reduced.	42
Figure 30. Oxidation process of sol-gel sample.....	44
Figure 31. Oxidation process of co-precipitation method.	45
Figure 32. Oxidation process of wet-impregnation sample.....	46
Figure 33. Oxidation process of mechanical mixing sample.....	47
Figure 34. Oxygen carrier with titanium(IV) oxide operated red-ox cycles at 950°C.	49
Figure 35. Oxygen carrier with titanium(IV) oxide in 45 red-ox cycles.	50
Figure 36. Oxygen carrier with titanium(IV) oxide from sol-gel method operated in 8 red-ox cycles.....	51
Figure 37. Oxidation kinetics.....	52
Figure 38. Reduction kinetics.	53

LIST OF TABLES

Table 1. Reactivity of different oxygen carriers and selection of the most promising carriers.....	9
Table 2. Crushing strength (N/mm) of the studied extrudates.....	14
Table 3. Solid-state reaction rate equations.....	29
Table 4. Data of repeat copper(II) oxide reduction.....	36
Table 5. Dispersion comparison between different methods.....	37
Table 6. Elemental ratio of area 1 in figure 26.....	38
Table 7. Elemental ratio of area 2 in figure 26.....	39
Table 8. Elemental ratio of average area in figure 26.....	39
Table 9. Oxidation comparison between different preparation methods.....	48

PREPARATION OF COPPER-BASED OXYGEN CARRIER SUPPORTED ON TITANIUM DIOXIDE

Yaowen Cui

August 2012

63 Pages

Directed by: Wei-Ping Pan, Yan Cao, Bangbo Yan and Rui Zhang

Department of Chemistry

Western Kentucky University

Chemical-looping combustion is an indirect oxygen combustion strategy, considered to be the most cost-effective power generation technology with the CO₂ inherently concentrated. In this process, a solid oxygen carrier is used to transfer oxygen from the air reactor to the fuel reactor, which completely isolates nitrogen in air to meet with fuels. The oxygen carriers in the combustion process are subjected to the severe environments, such as high temperatures, multi-cycle operations, and thermodynamic limitations. Thus, the preparation of an oxygen carrier with high durability and better kinetics under harsh environment could be an essential part of Chemical-looping combustion development. In this study, modified wet impregnation and co-precipitation methods have been developed. The active ingredient is copper(II) oxide, and the supporting material is either directly from titanium(IV) oxide (anatase 99%) or that prepared from other titanium resources such as titanium tetrachloride and tetrabutyl titanate. Preliminary results showed the prepared oxygen carriers functioned properly in the multi-cycles of oxidization and reduction in TGA at different temperatures. Characterization of used oxygen carriers was carried out using techniques of XRD, and SEM-EDS, which provide information for the difference between oxygen carriers from different preparation methods. Through the comparison, the oxygen carrier from the sol-gel preparation method has better dispersion and oxidation activity than those from mechanical mixing, wet-impregnation, and co-

precipitation method. Moreover, towards the oxygen carrier from sol-gel method, nucleation model and diffusion models were determined at different reaction periods.

1. Introduction

1.1 Objective

This study investigates the performance of titanium(IV) oxide as the supporting material of copper-based oxygen carrier from sol-gel method. In previous oxygen carrier research, many factors were studied, such as material (copper, nickel, iron, and so on), supporting materials (aluminum oxide, zirconium dioxide, silicon, and titanium(IV) oxide), active material ratio, and operational conditions. In this study, titanium(IV) oxide was used as the supporting material and the effects of different preparation methods, especially from sol-gel preparation method, were studied. Following preparation, the samples from different methods were evaluated with Thermogravimetric Analyzer (TGA), Simultaneous Differential scanning calorimeter and Thermogravimetric analyzer (SDT), and by comparison their chemical and physical properties were characterized with X-Ray Diffraction (XRD), and Scanning Electron Microscope (SEM).

1.2 Chemical-Looping Combustion (CLC)

1.2.1 Background

Global Warming

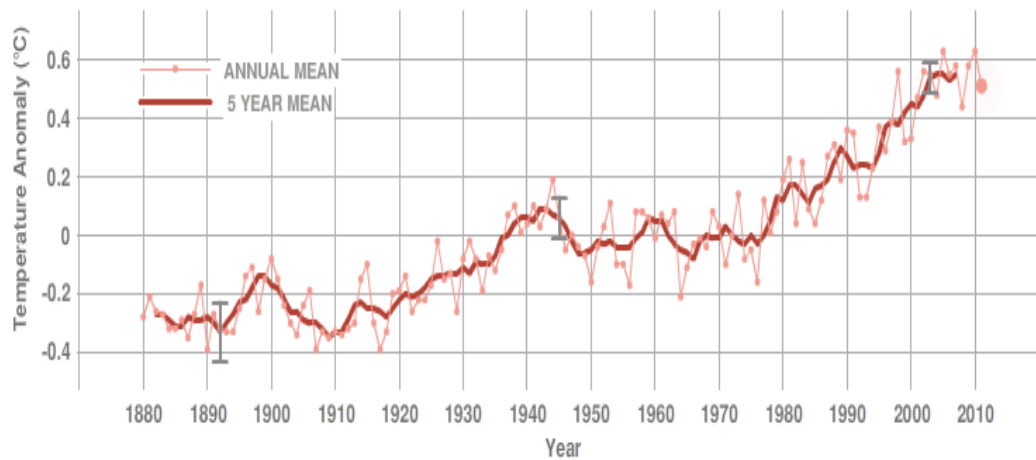


Figure 1. Surface temperature change of the earth from 1880 to 2010¹.

From the last century on, human beings have been facing the global warming issue and along with a series of problems related to global warming, such as sea level rising, land ice and Arctic sea ice decreasing, and other serious issues. Figure 1 illustrates the change in global surface temperature from 1880 to 2010 relative to 1951 to 1980 average temperature. The gray error bars represent the uncertainty of measurement. Figure 1 illustrates how the global surface temperature is increasing. Previous global warming research had linked the rising global surface temperature with human activity, especially activity resulting in carbon dioxide emission²⁻⁴.

Carbon dioxide is an important heat-trapping (greenhouse) gas. It acts as a blanket around the earth which prevents the release of heat. This effect is the so-called “greenhouse effect”. The rising level of greenhouse gas in the atmosphere results in the earth absorbing more solar energy and the increase in the earth surface temperature.



Figure 2. Atmospheric CO₂ concentrations in the air⁴.

Since industrialization, humans have known how to utilize fossil fuel to produce energy and do work. More and more carbon dioxide has been released to the atmosphere from fossil fuel combustion. Figure 2 shows atmospheric carbon dioxide in the air between 1950 and the present. The current level of carbon dioxide is much higher than the trend prior to 1950.

Coal Combustion

In the modern world, coal is still the most common energy source for electricity generation. Coal-fired power plants provided 44.8% of the electricity required in the U.S in 2010. According to the U.S. Energy Information Administration (EIA)⁵, natural gas and nuclear sources provided approximately 24.2% and 19.4% of total electricity generated, respectively. At this point, coal still cannot be replaced by other sources.

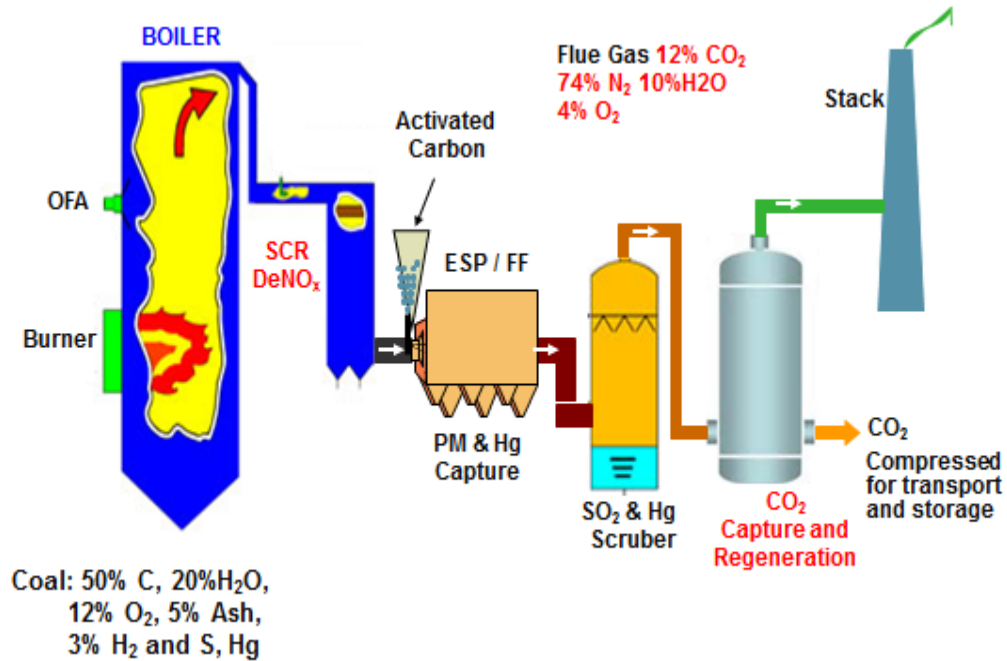


Figure 3. The layout of green coal combustion process.

Figure 3 is the layout of a solution of cleaning coal fired power plant. Flue gas is the product of combustion after sulfur oxide, mercury, and NO_x elimination process from fossil fuel which can be released to the open air through the stack. Its main component is nitrogen. Nitrogen is unreacted in the combustion process and comprises a large volume of the flue gas. It also contains carbon dioxide, a major greenhouse gas presently. In Figure 3, the amount of carbon dioxide in the flue gas is only 12%. Therefore, before storage, there should be a separation process to concentrate the carbon dioxide.

Carbon Dioxide Capture

In order to eliminate or minimize carbon dioxide emission from energy generation by a fossil-fuel power plant, several carbon dioxide capture processes have already been designed.

Post-combustion (pulverized coal combustion): In this process, coal is pulverized before combustion resulting in higher combustion efficiency. The flue gas contains NO_x,

SO₂, carbon dioxide, nitrogen and some unreacted oxygen. Carbon dioxide is separated from nitrogen. Either by chemical absorption, such as monoethanolamine (MEA) absorption or by carbon dioxide capture is utilizing membrane gas separation technology⁶.

Pre-combustion (Gasification): In a pre-combustion process, fuels are first converted into a mixture of carbon dioxide and hydrogen through either gasification (coal) or a reforming (nature gas) process. The product of gasification is called syngas; it contains carbon monoxide and hydrogen. Chemical and physical absorption processes are employed for carbon dioxide capture for pre-combustion process. The solvent as absorbent can be MEA as with the chemical method mentioned previously or pressure swing adsorption.

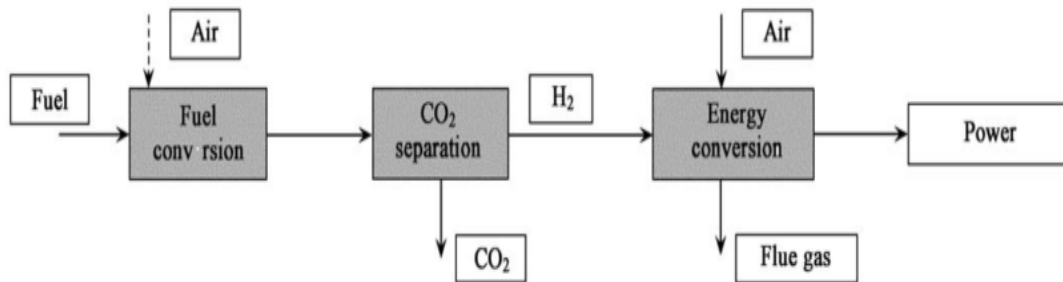


Figure 4. Gasification carbon dioxide capture process⁷.

Oxy-combustion: In oxy-combustion, high purity oxygen is separated from air. This pure oxygen replaces air as an oxidant to participate the combustion to produce pure carbon dioxide. After further SO₂ removal, the exhaust gas stream is approximately 90% carbon dioxide by volume on a dry basis. Therefore, the advantage of this method is saving the processes NO_x control and carbon dioxide separation. However, the cost for oxygen purification from air is a problem.

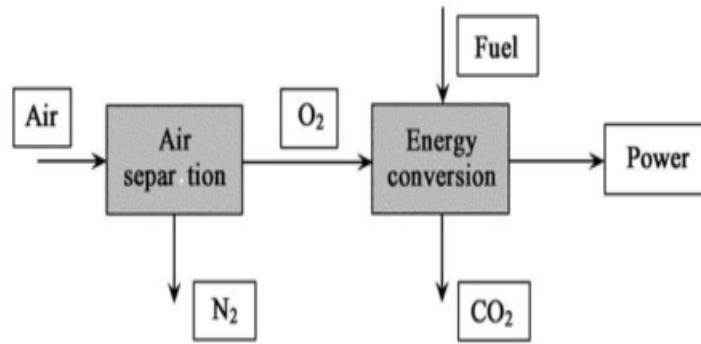


Figure 5. Oxy-firing carbon dioxide capture process⁷.

Though these three methods offer many advantages, the carbon dioxide separation processes would lead to high energy penalty and money cost.

1.2.2 Chemical-Looping Combustion

Chemical-looping combustion (CLC) is a novel and promising process with inherent carbon dioxide capture. It is also called unmixed combustion since it avoids directly mixing fuel and air. In the CLC process, nitrogen is not released with the flue gas.

The theory of chemical-looping combustion is shown in Figure 6. The whole chemical-looping combustion process can be separated into two sections. One is an air reactor and the other is a fuel reactor. A metal is oxidized in the air reactor to produce the metal oxide. The metal oxide is called the oxygen carrier. The oxygen carrier donates the oxygen in the fuel reactor to the fuel. The process is considered fuel combustion. The reduced metal is then transferred back to the air reactor ready to perform the next cycle. Oxygen carriers transport oxygen from the air to the fuel; meanwhile nitrogen is not released with the carbon dioxide.

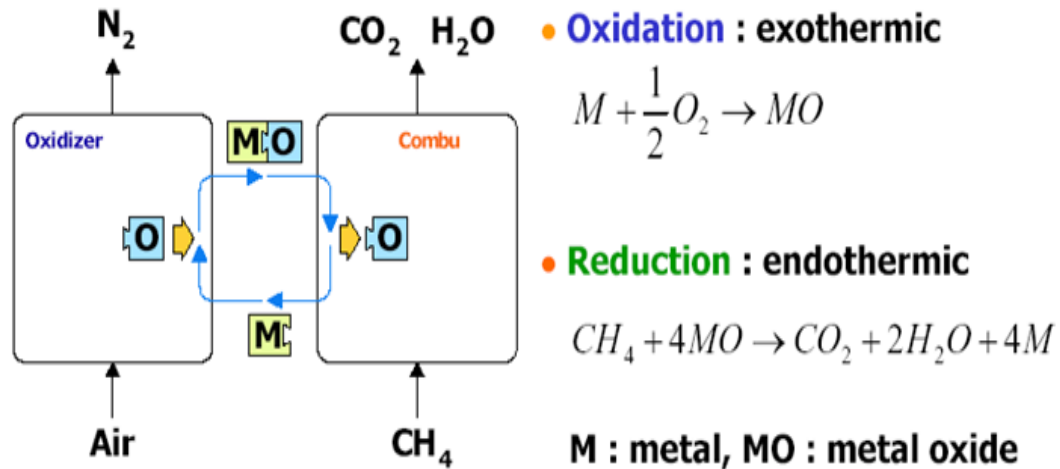
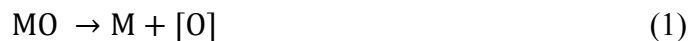


Figure 6. The theory of chemical-looping combustion.

In Figure 6, methane is used as an example to show the oxidation and reduction reaction functions. The energy released or absorbed depends on the change of enthalpy for the reactions. Normally the oxidation reaction is a strongly exothermic reaction, and reduction reactions are usually endothermic. However, when the oxidation process combines with the enthalpy of fuel oxidation by the oxygen donated from oxygen carrier, it could be exothermic. The separated functions are as follows:



The advantages of the CLC process:

- (1) With chemical-looping combustion, no carbon dioxide separation processes are required. This saves energy and money spent on reducing greenhouse gas emission to the atmosphere and thus reduces the fuel exhausted by advanced fuel utilized efficiency.
- (2) The product gas of combustion is absolutely harmless to people. The product gas stream from the air reactor is just nitrogen and unreacted oxygen, which can be released

to the open air. The product stream from the fuel reactor mainly consists of carbon dioxide and water vapor, which is separated via a cooling system. Separated carbon dioxide can be stored for further treatment.

(3) A well designed chemical-looping combustion system should not produce NO_x because elemental nitrogen is not oxidized.

In principle, all fuel can be utilized in the chemical-looping combustion process. The current technology of chemical-looping combustion with gaseous fuel is more mature. Solid fuel utilized in chemical-looping combustion still has some challenges to deal with, such as the separation of ash and oxygen carrier, and bottom bed feeding of fuel.

1.3 Oxygen Carrier

Oxygen carriers typically used for chemical-looping combustion include nickel, iron, and copper, due to their good activity. But none of them were perfect; they all had their advantages and disadvantages.

Table 1. Reactivity of different oxygen carriers and selection of the most promising carriers⁸.

Inert	T _{int} (°C) MeO(%)	Metal-based oxygen carriers															
		Cu				Fe				Mn				Ni			
		950 red-oxid	1100	1200	1300	950	1100	1200	1300	950	1100	1200	1300	950	1100	1200	1300
Al ₂ O ₃	80	a-a	e-e			a-a	a-a	b-b	b-b	a-a	b-b	e-e		a-a	a-b*	a-b*	b-c*
	60	a-a	e-e			a-a	b-b	b-b	b-b	b-b	c-c	e-e		a-a	a-b*	b-c*	e-e
	40	a-a	e-e			a-a	a-a	b-b	b-b	c-c	e-e	e-e		a-a	b-c	c-c	e-e
Sepiolite	80	a-a				a-a	a-a			a-a	a-a			a-a	a-a	a-a	c-c
	60	a-a				a-a	a-a			a-a	a-a			a-a	a-a	b-b	
	40	a-a				a-a	a-a			a-a	c-e			a-a	b*a	e-e	
SiO ₂	80	a-a				b-b	b-b			a-a	b-b			a-c*	a-c*	a-c*	a-b*
	60	a-a				a-a	b-b			a-a	e-e			a-c*	a-d	a-d	a-c
	40	a-a				a-a	a-a			a-a	c-e			a-c*	b-d	c-d	
TiO ₂	80	a-a				a-a	b-b	b-c*	b-c*	b-b	b-b			a-b*	a-b*	a-b*	b*-c*
	60	a-a				a-a	b-b	b-c*	c-c	e-e	e-e			a-a	a-a	a-a	a-b*
	40	a-a				a-a	b-c*	b-c*	b-d	e-e	e-e			a-a	a-a	a-a	a-b*
ZrO ₂	80	a-a				a-a	a-a	a-a	b-b	a-a	a-a	a-a	a-b*	a-c*	a-c*	a-d	a-d
	60	a-a				a-a	a-a	a-a	b-b	a-a	a-a	a-a	a-b*	a-b*	a-b*	a-b*	a-b*
	40	a-a				a-a	a-a	a-a	b-b	a-a	a-a	a-a	b*-b*	a-b*	a-b*	a-b*	a-b*

a = High reactivity and high conversion (X > 0.8 in 1 min)
 b = Conversion between 0.5-0.8 in 1 min.
 c = Conversion between 0.3-0.5 in 1 min.
 d = Conversion lower than 0.3 in 1 min but higher than 0.3 in 20 min.
 e = Low reactivity or low conversion (X < 0.3 in 20 min).
 * = Reach high conversion at long time

 Melt or decompose
 Low reactivity or crushing strength
 Selected particles by mechanical strength and reactivity

Nickel

Nickel was the first metal used for CLC. Even though bulk nickel can transport more oxygen than nickel supported on an inert binder, pure NiO displays poor re-oxidation over repeated reduction and oxidation cycles because of its agglomeration.

Thus, most papers reported a preference for supported nickel-based oxygen carriers. The supporting material, aluminum oxide, for nickel-based oxygen carriers attracted much attention. It can tolerate high temperatures by forming nickel oxide-aluminum oxide (NiAl₂O₄).

However, nickel combined with supporting material does not donate its oxygen to combustible gas, which is found by X-ray Diffraction (XRD). The formation of nickel

aluminate decreases the activity of nickel-based oxygen carriers during the reduction/oxidation.

Ni/MgAl₂O₄ as nickel-based oxygen carriers were also reported¹⁰. The addition of Mg limits the sintering of nickel oxide and stabilizes the nickel oxide, so that increasing the operating temperature to 1300°C. All investigated particles of NiO/NiAl₂O₄, NiO/MgAl₂O₄ and NiO/ZrO₂ showed high rates of reduction with no sintering tendencies during reaction and limited or no particle breakage^{11, 12}.

Even though nickel has many advantages, nickel is potentially hazardous; long-term inhalation of NiO is damaging to the lungs, causing lesions and in some cases cancer¹³.

Iron

Iron is possibly the most common and cheapest material available in nature. This makes iron an attractive choice for CLC. Hematite, a mineral form of Iron(III) oxide, is a non-porous smooth textural material of low surface area. Upon being exposed to continuously reduction-oxidation, the surface of the particles changes to a coarser texture with cracks and fissures.

After adding supporting material, the performance of the iron-based oxygen carrier increased substantially^{14, 15}. Hematite reactivity during the reduction process analysis shows that hematite reduction to magnetite is the fastest step. Subsequent steps, magnetite to ferrous oxide and ferrous oxide to iron, are much slower. From this it can be concluded that in an iron supported material, the hematite conversion to magnetite is the dominant chemical transformation.

Copper

Copper has several favorable features over other oxygen carrier common materials such as nickel and iron. These features include: (i) Cu-based oxygen carriers are highly reactive in both reduction and oxidation cycles, (ii) CuO reduction is favored thermodynamically to reach complete conversion using gaseous hydrocarbon fuels (e.g. methane), (iii) Cu-based oxygen carriers reduction and oxidation reactions are both exothermic, eliminating the need of energy supply in the reduction reactor, (iv) Cu is considered one of the cheapest metals that can possibly be used in CLC¹⁶.

Since copper-based oxygen carriers have high activity on both reduction and oxidation processes, CLC can be operated at a relatively lower temperature. Dr. Yan Cao and his co-workers⁹ studied a fluidized bed CLC process at 600°C using gasified solid fuels along with CuO. No particle agglomeration was observed although Cu₂O was found in the XRD analysis. The formation of Cu₂O was attributed to the decomposition of CuO.

Due to the uncoupling of copper, the release of oxygen provides the solid fuel chemical-looping combustion a solution. For solid fuel chemical-looping combustion, the connection between oxygen carrier and fuel is a problem. For the gaseous fuel, combustible gas can arrive to the surface of particles and even every pore of oxygen carrier, but for solid fuel such as coal, char, and charcoal, the contact area is much lower than gas.

Copper(II) oxide can decompose at high temperatures. This unique characteristic makes copper preferable over other materials as an oxygen carrier. However, the low melting point of copper and copper(II) oxide results in severe agglomeration problems.

Despite so many advantages from copper-based oxygen carriers, it still has not received much notice due to severe agglomeration from low melting point of copper (1085°C) and copper(II) oxide (1200°C).

Cu-based oxygen carriers showed a measurable crushing strength when using SiO₂ and TiO₂ as inert supports. Fe-based oxygen carriers showed high crushing strength values, especially those prepared with Al₂O₃, TiO₂, and ZrO₂ and sintered at temperatures above 1100°C.

Even though the supporting material does not participate directly in the reduction-oxidation cycle, its existence can improve the active components' performance. The ability of the metal to act as an oxygen carrier is dependent on the degree of metal loading and stability over repeated reduction oxidation cycles. Oxygen carrying ability is a major function of the metal loading and of the stability of the carrier over repeated reduction–oxidation cycles. In addition, different oxygen carriers may be reduced to different states depending upon the metal dispersed on the support materials. As a result of this, it is quite common to observe a reported mass-based conversion (oxygen ratio) to express the oxygen carrying capacity of a given carrier¹⁹.

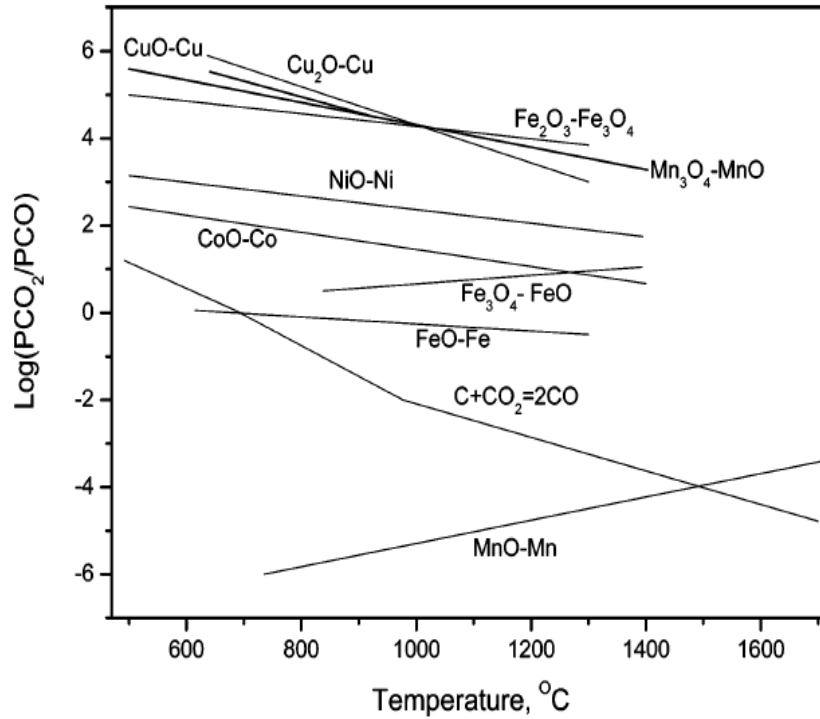


Figure 7. Variation of the thermodynamic equilibrium factor for $\text{Me}_x\text{O}_y\text{-CO}$ as a function of temperature¹⁸.

Figure 7 shows the plot of $\log(P_{\text{CO}_2}/P_{\text{CO}})$ versus temperature in the flue gas after the oxygen carrier triggered CLC. When carbon or fuel gas incompletely combusts, carbon monoxide gas will be produced. The heat generated from incomplete combustion is much lower than from complete combustion, so more carbon monoxide means less efficiency. Since carbon monoxide inhalation is dangerous, selection of the metal with the highest carbon dioxide conversion percentage is the obvious choice.

Supporting Material

When raw material is used as the oxygen carrier, many metals suffer from severe agglomeration. For instance, copper or copper(II) oxide has a relatively low melting point that causes copper-based oxygen carriers to tend to easily agglomerate. After agglomeration, the material adheres together, resulting in less surface area. The specific

surface area will apparently drop. Agglomeration results in incomplete combustion, oxygen carrier degradation, or increased reaction time.

Inert supporting material prevents agglomeration by dispersing the oxygen carrier. The raw material usually has low crushing strength, but a supporting material can increase the oxygen carriers' strength.

Table 2. Crushing strength (N/mm) of the studied extrudates¹⁹.

Inert	T _{um} (°C) MeO(%)	Metal-based oxygen carriers															
		Cu				Fe				Mn				Ni			
		950	1100	1200	1300	950	1100	1200	1300	950	1100	1200	1300	950	1100	1200	1300
Al ₂ O ₃	80	3	5		0	13	105	61	0	0	0		0	0	0	0	
	60	0	0		0	12	17	57	0	0	0		0	0	0	0	
	40	0	0		0	12	22	65	0	3	12		0	2	3	4	
Sepiolite	80	4			9	48			1	23*			0	1	4	120	
	60	0			7	20			1	12*			1	6	14*		
	40	0			1	14			0	27*			0	3	53		
SiO ₂	80	22			12	60			10	37			0	1	11*	25*	
	60	20			15	85			16	28			6	16	32	45	
	40	17			10	52			16	22			11	29	35		
TiO ₂	80	66			12	71	111	17	2	57			1	16	42	50	
	60	59			21	45	36	11	8	77			4	17	32	48	
	40	43			40	94	81	30	13	84			14	23	33	65	
ZrO ₂	80	6			3	25	33	76	0	11	37	29	0	2	1	3	
	60	2			12	20	29	54	1	16	33	25	0	0	3	5	
	40	1			13	19	19	56	2	11	36	27	0	3	13*	11*	

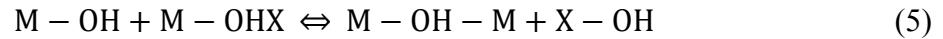
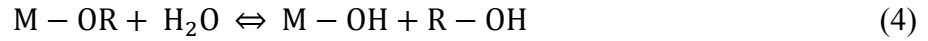
 Melt or decompose
 Soft (Values lower than 10 N/mm)
 * Broken after 5 cycles

1.4 Preparation Methods

A sol-gel method was proposed in 1968 by Nicolaon and Teichner²⁷. The sol-gel preparation method results in a continuous transformation of a solution into a hydrated solid precursor. It is widely applied because of its versatility. Through the sol-gel method, texture, composition, homogeneity, and structural properties of the product can be controlled²⁶.

The sol-gel method is based on the hydrolysis and gelation of alkoxides or other reactive compounds in alcohol solution. The sol-gel synthesis process can be expressed in the following sequence.

The hydrolysis of the metal alkoxides is as follows:



Where M=metal or silica; R=alkyl, X=H or R.

Through the sol-gel synthesis, a highly cancellated and metastable polymer can be prepared. In this open structure, the primary units are connected by chemical bonds, hydrogen bonds, dipole forces, or van der Waals interactions. After eliminating the liquid within the gel, this structure can be transferred to solid phase²⁸.

The sol-gel method can be used in oxygen carrier preparation²⁹. In this study, the gelation process happened in the methanol solution with dissolved copper(II) nitrate. So when the reticulated structure formed, the copper(II) nitrate existed between primary units of the gel. After liquid elimination, copper(II) nitrate was coated on the surface of solid phase titanium(IV) oxide. After calcination, nitrate decomposition produced a mixture of copper(II) oxide and titanium(IV) oxide.

2. Experimental

2.1 Preparation of Oxygen Carrier

The copper-based oxygen carriers supported by titanium(IV) oxide were prepared by four methods: mechanical mixing method, wet impregnation method, co-precipitation method, and sol-gel method.

2.1.1 Mechanical Mixing Method

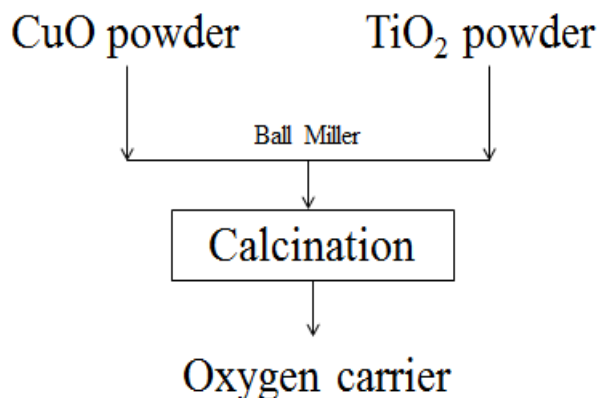


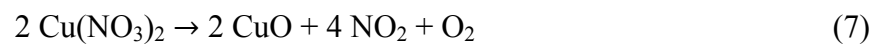
Figure 8. Process of mechanical mixing preparation method.

Copper based oxygen carriers supported on titanium(IV) oxide prepared using the mechanical mixing method were made from pure copper(II) oxide (prepared from copper(II) nitrate crystals) and titanium(IV) oxide (Titanium(IV) oxide, 99%, anatase powder, Acros organics). Copper(II) oxide (40%) and titanium(IV) oxide powder (60%) were added to a ball mill. After grinding in the ball miller for half an hour, the oxygen carrier precursor was made. Titanium(IV) oxide as anatase will transfer to rutile partially or completely over temperatures of 700 °C. To prevent the phase change from occurring during the CLC process, the mixture of copper(II) oxide and titanium(IV) oxide was calcinated at 800°C for 3 hours.



Figure 9. Ball mill.

Copper(II) oxide was prepared from the decomposition of copper(II) nitrate. The reaction function is shown below:



2.1.2 Wet-Impregnation Method

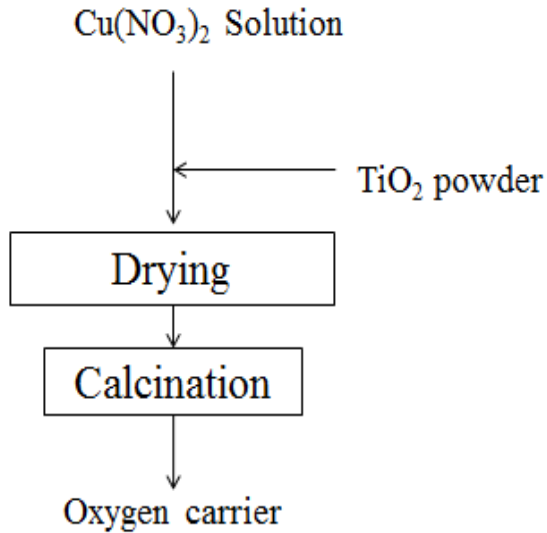


Figure 10. Process of wet-impregnation preparation method.

The wet-impregnation method used a fresh sample of oxygen carrier material. Titanium(IV) oxide powder (Titanium(IV) oxide, 99%, anatase powder, Acros organics) was used as an inert support. Anatase powder was dropped in to saturated copper(II) nitrate aqueous solution. In order to increase the solvent expanse rate, the solution was continuously stirred by a magnetic stirring apparatus. The impregnated sample was dried overnight and calcinated at 800°C in a tube furnace (Across International, KTL 1400) to decompose the copper(II) nitrate to copper(II) oxide. At 800°C titanium(IV) oxide is present in the rutile phase, the precursor was calcinated at 800°C in order to avoid potential phase changing during the operating process.

2.1.3 Co-Precipitation Method

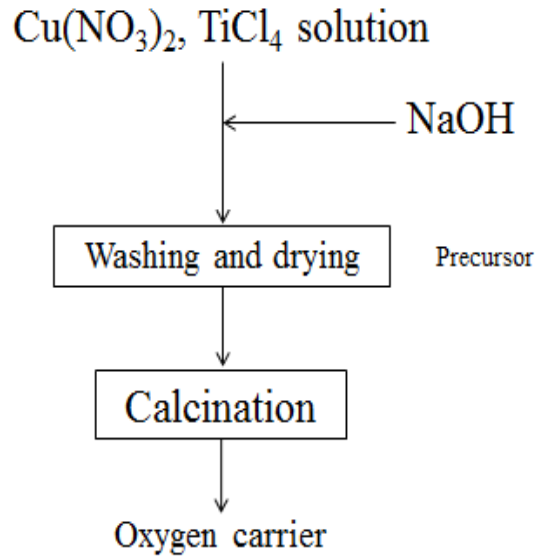


Figure 11. The process of co-precipitation preparation method.

Because titanium and copper ion can be precipitated in a basic environment, copper-based oxygen carriers with titanium(IV) oxide supports can be produced from a co-precipitation method. Copper(II) oxide and titanium(IV) oxide were from copper(II) nitrate and titanium tetrachloride, respectively. The solution of titanium tetrachloride was made first. Pure titanium tetrachloride is in the liquid phase at room temperature. Titanium(IV) oxide hydrolyzes and produces titanium(IV) oxide and hydrochloric acid. The reaction process is described below:



During the dissolving process, some 1 M hydrochloric acid solution was added to suppress hydrolysis. This solution can only be kept for a short time. Titanium ions will hydrolyse after a long time, decreasing the concentration of titanium in the solution and making it non-homogeneous.

Precipitation processes were performed on a magnetic stirrer at room temperature. For the copper-based oxygen carrier preparation, ammonia solution was utilized as

precipitant. The precipitant solution was added drop by drop into the beaker under mild agitation with a desired ratio of copper(II) nitrate and titanium tetrachloride aqueous solution, till the pH reached 8.0 which is measured by pH meter (Orion 3 star pH Benchtop, Thermo Electron Corporation). After 1 hour at 40°C, the resultant suspension was filtered, with suction, and washed four times with distilled water. The precipitated sample was then dried at 80°C in a drying box for 24 hours. The dried cake was crushed with a ball mill and calcinated at various temperatures (650°C, 800°C, and 1000°C) for 3 hours.

2.1.4 Sol-Gel Method

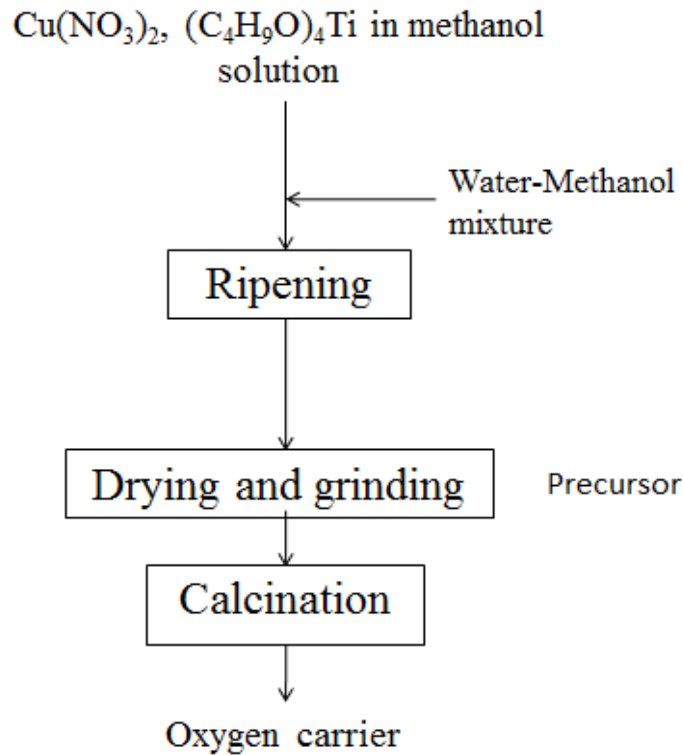


Figure 12. Process of sol-gel preparation method.

The titanium resource, tetrabutyl titanate (Titanium n-butoxide, 99%, Acros), has the ability to hydrolyze, forming titanium(IV) oxide of sol and gel. Depending on the

amount of water added to the solution, titanium(IV) oxide as binder of copper-based oxygen carrier can be prepared from the sol-gel method. The sol-gel preparation process was performed using a magnetic stirrer at room temperature. Tetrabutyl titanate was mixed with anhydrous methanol (Methyl alcohol, 99.8%, Acros) at a ratio of 1: 1 by weight in the beaker. A desired amount of copper(II) nitrate was added in the methanol solution. The water of crystallization in copper(II) nitrate was released to the solution, and promoted the hydrolysis of tetrabutyl titanate. After several minutes, the solution became sol and the magnetic stir rolled slower and slower. Until the stir stopped rolling, the gel of titanium(IV) oxide with copper(II) nitrate was formed. The mixture gel, after set in a water bath at 60°C for 1 hour as ripening time, was dried in drying box at room temperature for 24 hours. The dried sample was crushed to fine powder, then calcinated at various temperatures (650°C, 800°C, 1000°C, and 1350°C) for 3 hours.

Due to the sufficient amount of water crystallized in copper(II) nitrate, when preparing the oxygen carrier with low copper(II) oxide content, such as 5% or 20% copper(II) oxide ratio, extra water and methanol should be added to the solution to trigger hydrolysis of TBOT.



Figure 13. Across International KTL 1400 Tube Furnace.

2.2 Characterization

In order to study the crystalline phase of the titanium(IV) oxide and copper(II) oxide particles mixture, powder X-ray diffraction system (XRD) (Thermal electricity, Thermo ARL X'tra) with a Ni-filtered Cu K α radiation was used. The sample pattern was recorded in steps of 0.02° in the 2 θ range of 5° to 90° and with the speed of 0.6° per minute. The X-ray generator was set to 20kV and 20mA. Powder phase identification of the sample was made with the help of the XRD database in the software (Crystal Impact, version 1.11).



Figure 14. Thermo ARL powder X-Ray Diffraction.



Figure 15. The X-Ray beam and detector of XRD.

The oxygen carriers were analyzed using a JEOL JSM 5400LV scanning electron microscope. The instrument was operated in low vacuum mode at a chamber pressure of 110 milli-torr using a back-scatter in a electron detector. EDX apparatus connected with SEM was also used to do an elemental analysis to determine the ratio of every element in the mixture.



Figure 16. JSM-5400LV Scanning Electron Microscope.

Thermogravimetric Analysis was used to study the process of calcination. The precursors of oxygen carriers from various preparation methods were loaded into the TGA or the SDT, the temperature program was isothermal for 5 minutes to stabilize the system, and then ramp to 800°C at 10°C per minute, then hold at 800°C for 1 hour. All the tests were completed in an air atmosphere.

2.3 Performance Tests

In this study, a thermogravimetric Analyzer (TGA), TA type 2950, was used for oxygen carriers' activity tests. Figure 17 shows the TGA and the gas auto-switcher used. The furnace material was quartz rather than aluminum oxide, which would have been damaged from the reductive gas in experiments. Considering quartz since quartz is unstable at very high temperature, this furnace cannot be operated at over 1000°C for safety concerns. The sample holder was a platinum pan with low boundary, to minimize the effect from active gas diffusion resistance around the solid sample during the operation. The temperature and sample weight were recorded continuously by a computer running TA software <TA Universal Analyzer 2000>. Nitrogen flowed through the microbalance head to keep the electronic parts free of the reactant gas. The flow rate of the reacting gas mixture was controlled by an electronic mass flow controller (Aalborg, GFC) and entered the furnace through the upper parts of the quartz tube. For the reduction process, hydrogen (10% by volume) in helium acted as the reducing agent. Air was the oxidant in the oxidation process. The gas route is controlled by an automatic gas switch accessory (TA instrument), and then alternatively mixed with nitrogen before entering the furnace. The ratio of reactant gas before entering the furnace is 90% by volume.



Figure 17. TGA and gas auto-switcher system.

For the oxygen carriers' reactivity test, samples prepared using different methods were loaded on the platinum pan. About 40 mg oxygen carrier was loaded into the TGA. The temperature program was isothermal at room temperature for 5 minutes to get a stable weight and temperature. The sample was then heated to the desired temperature in a nitrogen atmosphere at 20°C per minute. After reaching the set temperature, the gas was switched to the hydrogen mixture (gas 1) to start the reduction process. The reduction time was set to 5 minutes. The nitrogen was used as a purge gas in between gas cycles to prevent mixing hydrogen and oxygen. After the nitrogen purge, the gas was switched to air (gas 2) into a furnace as an oxidant. The oxidation time varied according to the activity of the oxygen carrier from different preparation methods. The beginning of the reduction process through the end of the oxidation was considered as a reduction-

oxidation cycle. This cycle process was repeated many times. The system recorded the weight loss and temperature versus time.

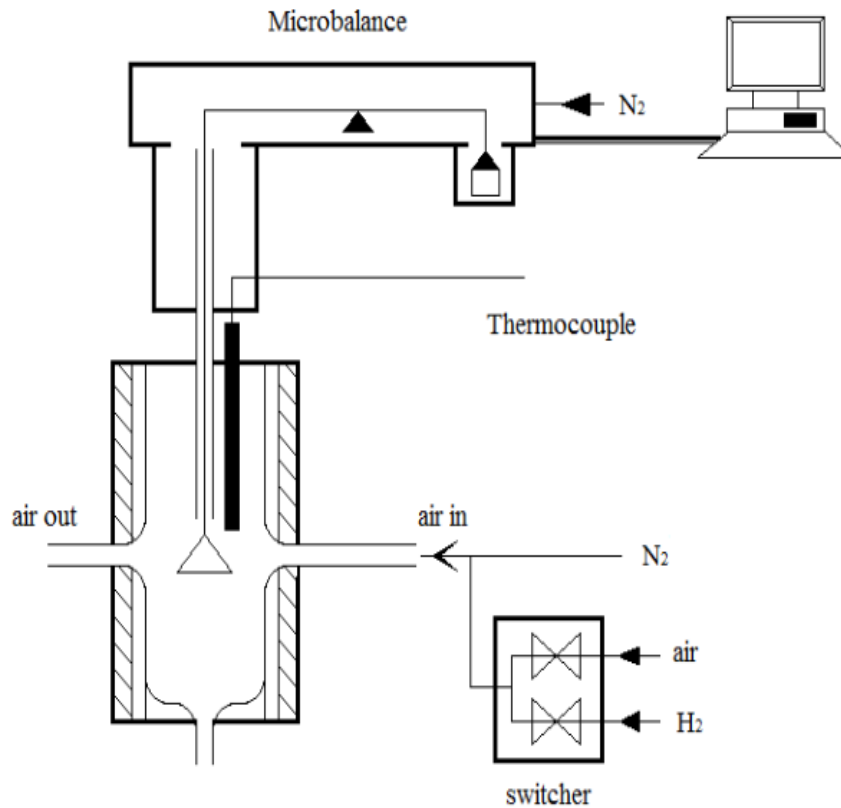


Figure 18. Schematic drawing of the thermogravimetric analyzer.

For the major activity tests of the oxygen carrier based on copper, the operational temperature was set at 800°C. This low temperature was used to prevent copper(II) oxide decomposition to copper(I) oxide.

2.4 Data Reduction Mathematics

2.4.1 Variance:

For the dispersion comparison, variance was utilized; the function of it is defined as below:

$$\sigma^2 = \frac{\sum (X_i - \bar{X})^2}{n-1} \quad (9)$$

Where X_i is the weight loss of a sample, and \bar{X} is the average of this series of samples.

2.4.2 Oxygen Capacity:

The capacity determines the ability of oxygen carrying, therefore represents the efficiency of the chemical-looping combustion process.

$$\text{Capacity} = \left(1 - \frac{M_{\text{red}}}{M_{\text{ox}}}\right) * 100\% \quad (10)$$

Where M_{red} is the molar weight of the reduced oxygen carrier after the reaction; M_{ox} is the molar weight of the oxidized oxygen carrier after the reaction.

2.4.3 Conversion:

The conversion of the reaction during the red-ox cycle process was defined as follows:

$$\text{Reduction: } X = \frac{m_{\text{ox}} - m}{m_{\text{ox}} - m_{\text{red}}} \quad (11)$$

$$\text{Oxidation: } X = \frac{m - m_{\text{red}}}{m_{\text{ox}} - m_{\text{red}}} \quad (12)$$

Where m , m_{red} , and m_{ox} represent the weight of sample, totally reduced, and fully oxidized.

2.5 Kinetics

To study the process of reduction and oxidation reactions, the general expression of isothermal reactions was introduced. Hancock and Sharp²⁰ had described a method with kinetics of isothermal solid-state reactions based on an equation that describes the nucleation and growth processes. A function between conversion and time was made as follows:

$$X = 1 - \exp(-at^b) \quad (13)$$

$$\ln(-\ln(1-X)) = \ln a + blnt \quad (14)$$

where a and b are both constants. Parameter a is partially according to the nucleation frequency and rate of grain growth, and b is varied with the geometry of the system. The constants a and b are determined by the Hancock and Sharp plot^{22, 23, 24}.

Table 3. Solid-state reaction rate equations²¹.

Function	Equation	Value of b
D ₁ (X)	X ² =kt	0.62
D ₂ (X)	(1-X) ln(1-X)=kt	0.57
D ₃ (X)	[1-(1-X) ^{1/3}] ² =kt	0.54
D ₄ (X)	1-2X/3-(1-X) ^{2/3} =kt	0.57
F ₁ (X)	-ln(1-X)=kt	1.00
R ₂ (X)	1-(1-X) ^{1/2} =kt	1.11
R ₃ (X)	1-(1-X) ^{1/3} =kt	1.07
Zero order	X=kt	1.24
A ₂ (X)	[-ln(1-x)] ^{1/2} =kt	2.00
A ₃ (X)	[-ln(1-X)] ^{1/3} =kt	3.00

Table 3 shows the solid-state reaction equations. The function D₁(X) to D₄(X) refers to some important diffusion equation. F₁(X) is the function for a first-order reaction. R₂(X) and R₃(X) are, respectively, the equations of phase-boundary-controlled reactions for a cylinder or a circular disk and a sphere. A₂(X) and A₃(X) are equations referred to nucleation process for b = 2.0 and 3.0, respectively.

3. Result and Discussion

3.1 Preparation Factors

3.1.1 Calcination Temperature

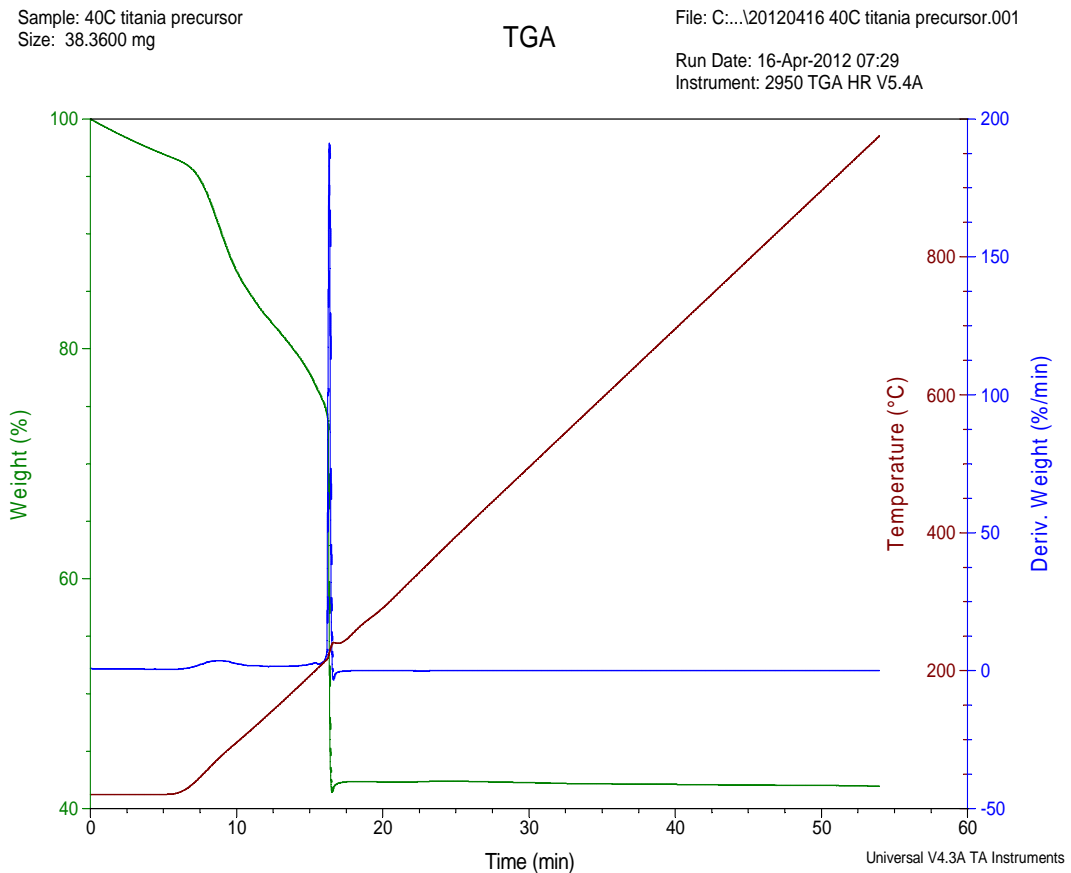


Figure 19. TGA plot of precursor of the sample calcination.

Figure 19 shows the weight loss profile for the oxygen carrier precursor from the sol-gel method. The temperature program for the TGA was isothermal for 10 minutes; then heated to 1000°C at 20°C per minute in an air atmosphere. The precursor was dried at 40°C in a drying oven over night and then crushed in a ball mill. The phase of the

mixture should be copper(II) nitrate and titanium(IV) oxide with some organic material produced in the hydrolysis process. As the temperature rose, the organic material such as butyl alcohol was released firstly. At the beginning of the isothermal stage, the versatile material in the precursor became active and started to escape from the mixture. When the temperature continued to rise, the versatile compound evaporated faster than during isothermal period. At 230°C, the copper(II) nitrate in the precursor started to decompose.

At 300°C, both the decomposition of copper(II) nitrate and the evaporation of the versatile compound finished and the weight loss stopped. At this point, the sample in the TGA consisted of a mixture of copper(II) oxide and titanium(IV) oxide.

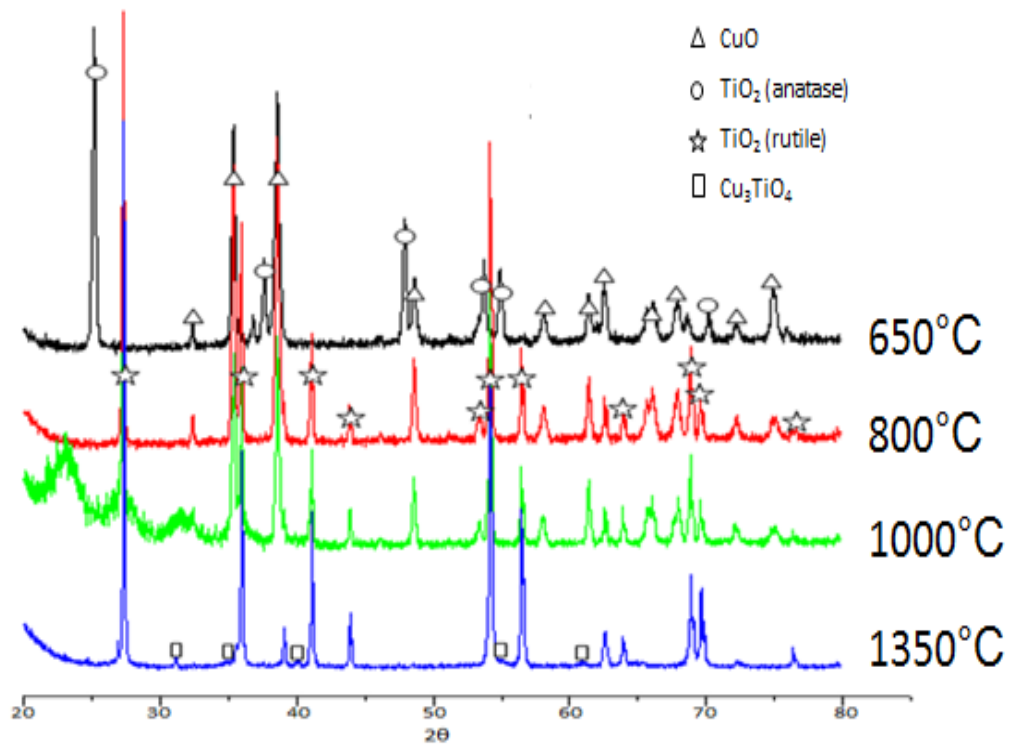


Figure 20. XRD pattern of oxygen carrier calcinated from different temperature.

In Figure 20, the XRD pattern shows that the precursor of oxygen carrier was calcinated in a tube furnace with 650°C, 800°C, 1000°C, and 1350°C. The pattern of these oxygen carriers shows a binary system, copper(II) oxide and titanium(IV) oxide.

Phase change according to the calcination temperature. At 650°C, the oxygen carriers were a mixture of copper(II) oxide and titanium(IV) oxide, and the phase of titanium(IV) oxide was anatase. There was no combination between copper(II) oxide and titanium(IV) oxide. At 800°C, titanium(IV) oxide of anatase transferred to rutile; there is no evidence to support an interaction between copper and titanium. At 1000°C, the pattern was very similar to the pattern at 800°C. When the temperature reached 1350°C, exceeding the melting point of copper(II) oxide, some of the copper(II) oxide was lost from the oxygen carrier, so that the peaks of the copper were very tiny. The peaks from the copper(II) titanate still can be distinguished, including that copper(II) oxide had combined with titanium(IV) oxide at 1350°C to produce copper(II) titanate.

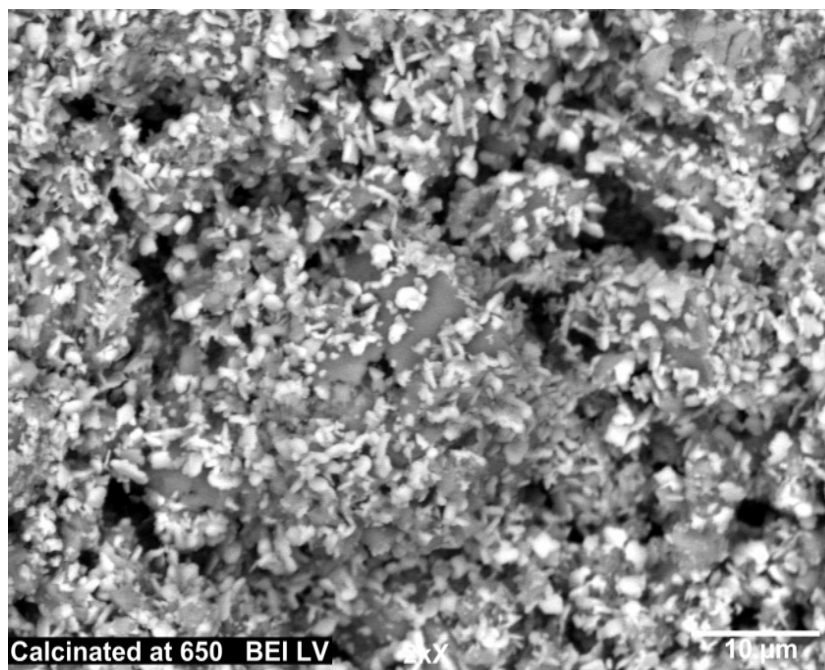


Figure 21. Oxygen carrier calcinated at 650°C.

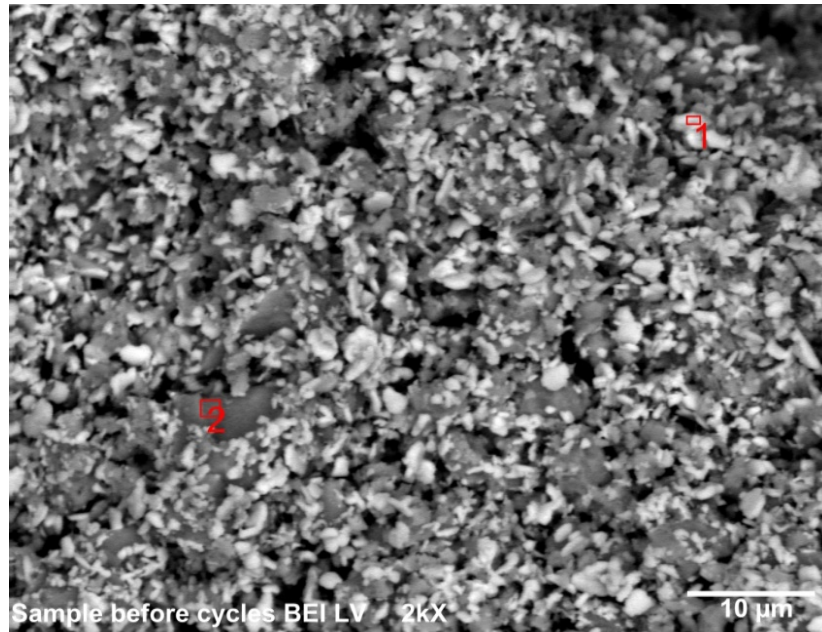


Figure 22. Oxygen carrier calcinated at 800°C.

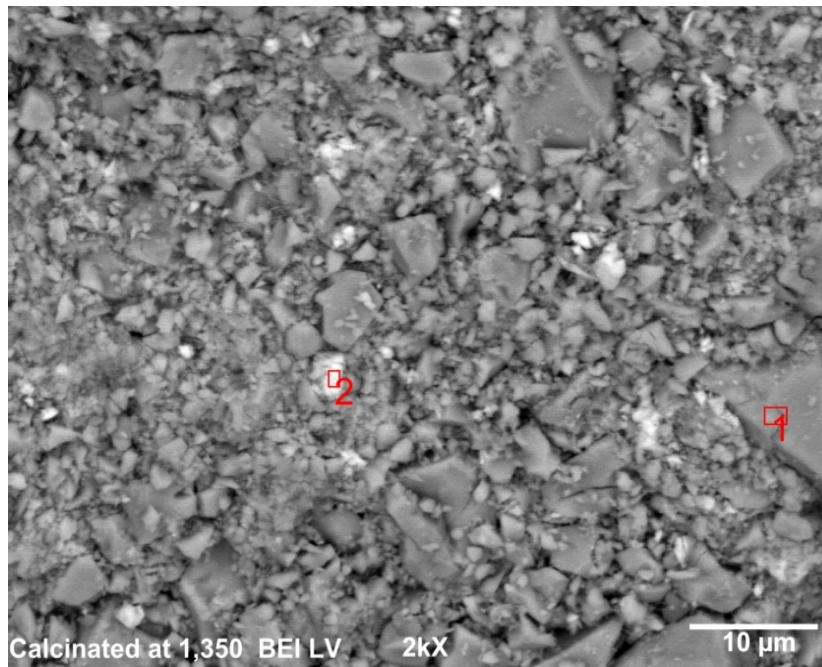


Figure 23. Oxygen carrier calcinated at 1350°C.

The SEM pictures shown in figure 21 to 23 show the microscopic morphology of the oxygen carriers calcinated at different temperatures at 2000 times' magnification. The 650°C and 800°C images show clearly distinguishable bright and dark areas, they refer to

higher copper loading and lower area, respectively. In the 1350°C SEM image, the bright area is very small. The melting point of copper(II) oxide is 1026°C; during the calcination process, copper(II) oxide melted and sank to the bottom of the crucible due to gravity. The dark areas refer to titanium(IV) oxide.

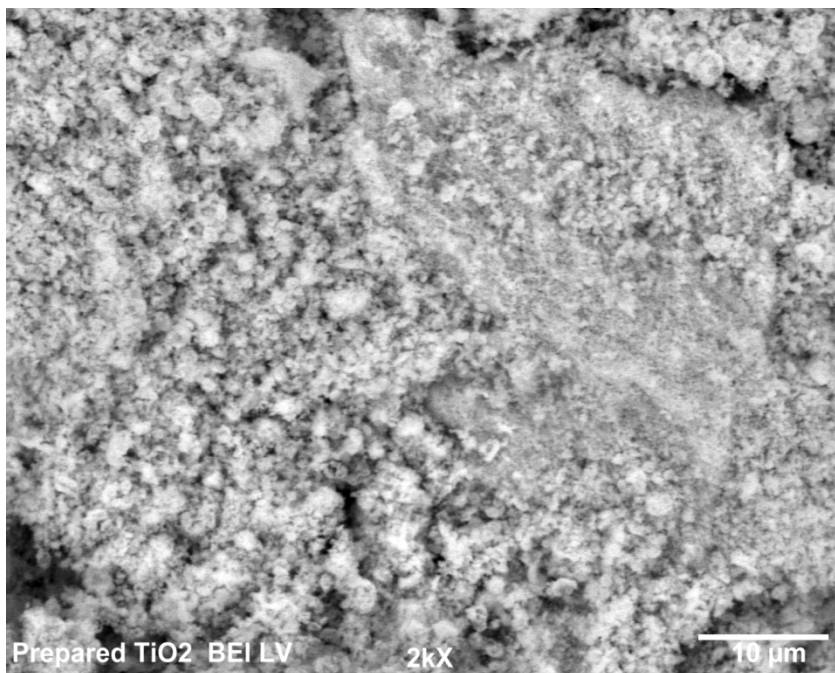


Figure 24. SEM picture of prepared titanium(IV) oxide.

Figure 24 shows the SEM image of pure titanium(IV) oxide prepared from the sol-gel method and calcinated at 800°C

3.1.2 Dispersion

In order to study the difference between oxygen carriers from different preparation methods, the concept of variance in statistics was employed. The samples of copper(II) oxide were reduced in TGA to measure the weight loss during the reduction process. The dispersion between samples was calculated using the variance of this data. Lower sample variance indicates better copper(II) oxide dispersion.

The samples from different preparation methods were shaken and divided into 10 equal parts. They were then subjected to reducing conditions in the TGA. Following the reduction reaction, the weight loss can be measured by the TGA. The molar weight of copper(II) oxide and titanium(IV) oxide are very close, 79.89 gram per mole and 79.86 gram per mole respectively. Since the weight loss was from the oxygen donated from copper(II) oxide (20% by weight), the copper(II) oxide loading of the oxygen carriers can be approximately calculated as 5 times the percentage weight loss of the oxygen carrier during the reduction process. Therefore, the copper(II) oxide loading of different samples can be compared. The weight loss data during reduction from TGA is shown in Table 4.

Table 4. Data of repeat copper(II) oxide reduction.

Method	Mechanical Mix(Bottom)	Wet-Impregnation	Co-precipitation	Sol-Gel
	8.81	8.28	8.16	8.53
	9.05	8.23	8.14	8.56
	9.1	8.24	8.24	8.56
	9.39	8.27	8.26	8.59
Weight Lost	8.94	8.25	8.35	8.61
(%)	9.05	8.41	8.18	8.65
	8.93	8.32	8.24	8.64
	9.01	8.24	8.22	8.67
	8.86	8.34	8.15	8.61
	9.15	8.25	8.23	8.55

Table 5. Dispersion comparison between different methods.

Method	Mechanical Mix (Bottom)	Wet-Impregnation	Co-precipitation	Sol-Gel
Weight Lost	9.03	8.28	8.22	8.60
Average/mg				
Copper(II) Oxide Ratio/%	45.14	41.19	41.09	42.99
Variance	0.25	0.03	0.04	0.02
Standard Deviation	0.50	0.17	0.2	0.14

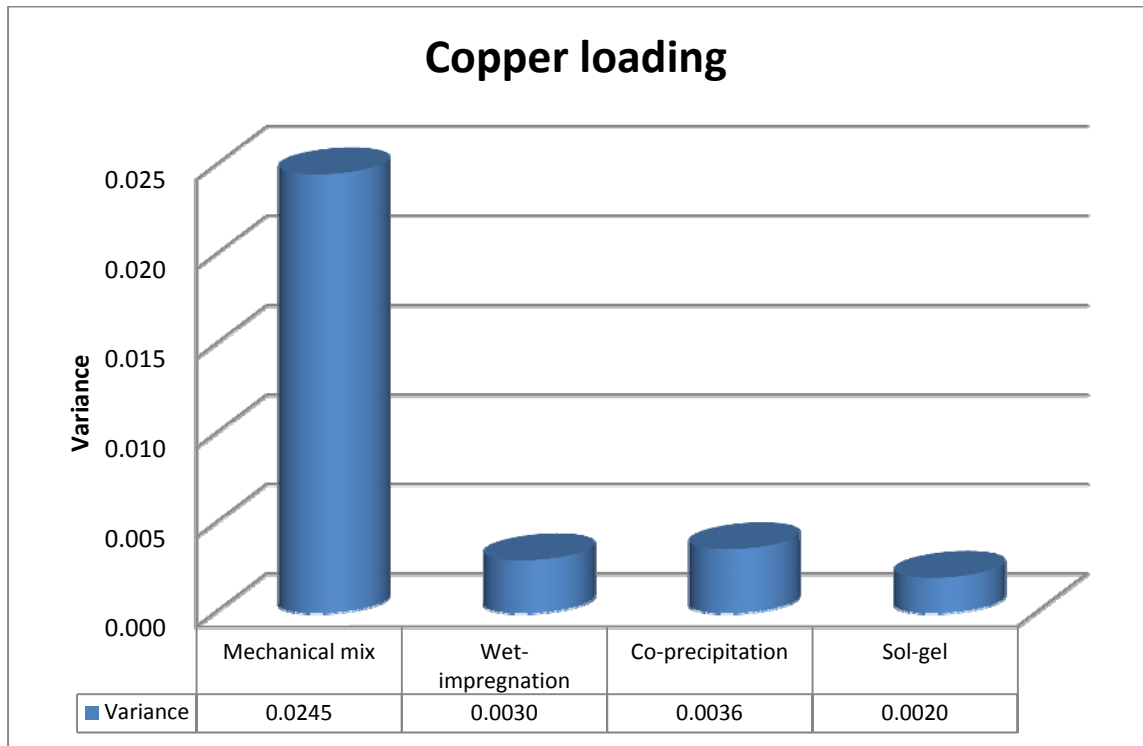


Figure 25. Dispersion of oxygen carrier prepared from different method.

From tables 4, 5, and figure 25, the oxygen carriers from the sol-gel method had the least variance and smallest standard deviation compared with the mechanical mixing method, wet-impregnation and co-precipitation methods. Therefore, the sol-gel method has better copper(II) oxide dispersion loading than the other two preparation methods.

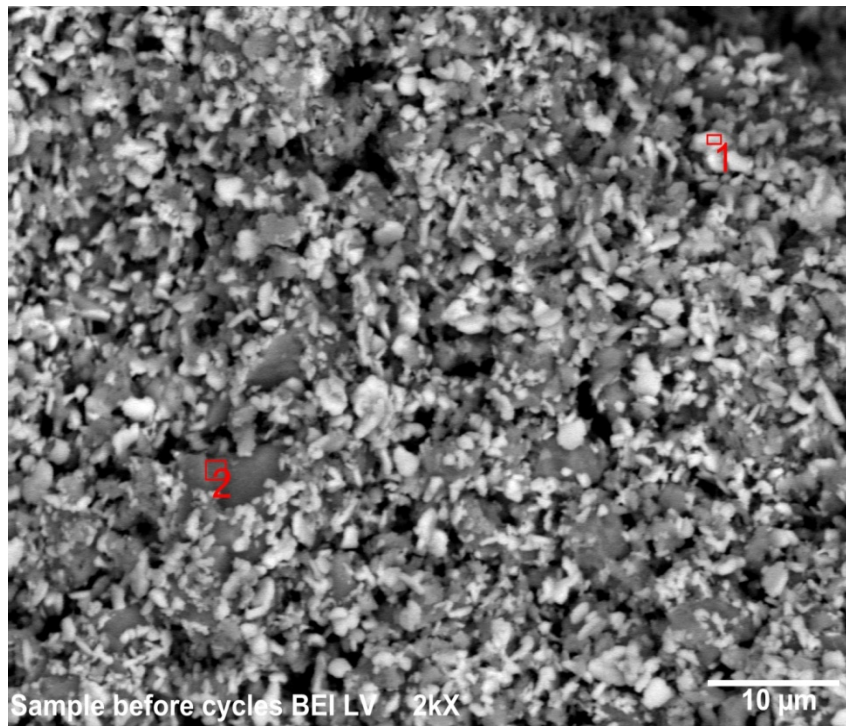


Figure 26. Oxygen carrier calcinated at 800°C.

Table 6. Elemental ratio of area 1 in figure 26.

Elt.	Line	Intensity (c/s)	Error 2-sig	Atomic %	Conc	Units	
O	Ka	45.06	2.717	62.46	30.90	wt.%	
Ti	Ka	88.03	3.616	9.58	14.17	wt.%	
Cu	Ka	129.79	4.280	27.96	54.93	wt.%	
				100.00	100.00	wt.%	Total

Table 7. Elemental ratio of area 2 in figure 26.

Elt.	Line	Intensity (c/s)	Error 2-sig	Atomic %	Conc	Units	
O	Ka	22.34	1.850	66.31	37.90	wt.%	
Ti	Ka	235.45	5.709	25.65	43.85	wt.%	
Cu	Ka	36.30	2.348	8.04	18.25	wt.%	
				100.00	100.00	wt.%	Total

Table 8. Elemental ratio of average area in figure 26.

Elt.	Line	Intensity (c/s)	Error 2-sig	Atomic %	Conc	Units	
O	Ka	6.05	1.036	52.02	24.37	wt.%	
Ti	Ka	89.90	3.538	29.69	41.62	wt.%	
Cu	Ka	27.55	2.003	18.28	34.01	wt.%	
				100.00	100.00	wt.%	Total

Though the sol-gel method provides relatively good dispersion of the oxygen carrier, the copper(II) oxide is not loaded evenly on the titanium(IV) oxide. Figure 26 shows particles from the sol-gel method magnified 2000 times.

From the figure 26, bright and dark areas refer to different copper(II) oxide ratios and can be distinguished clearly. With SEM, electrons are shot towards the atom, with heavier atoms attracting more and more electrons. The atomic weight of copper is larger than titanium, so the bright areas correspond to copper. The average elemental ratio was

shown in Table 8 and the copper ratio is 34%, so that the copper(II) oxide loaded was 41% by weight. For the bright spot (area 1 in Table 6) its copper elemental ratio is 54% by weight, and copper(II) oxide ratio is 65%. The dark place (area 2 in Table 7) contained 18% copper and therefore 22% copper(II) oxide.

3.2 Titanium(IV) Dioxide Versus Alumina Supporting

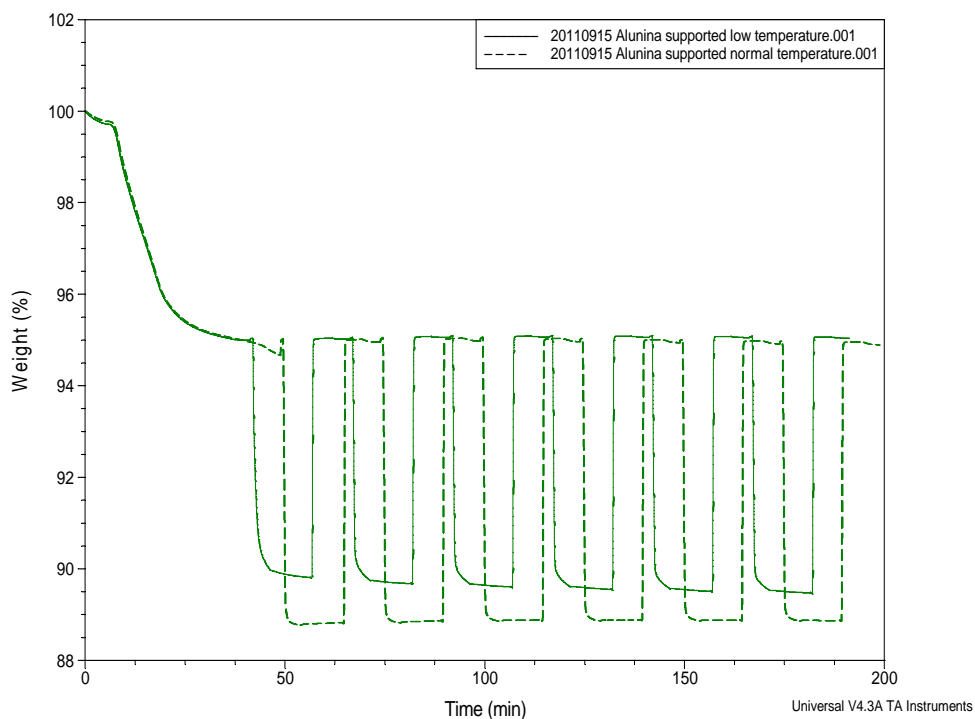


Figure 27. Alumina as an oxygen carrier support at 650°C (solid line) and 800°C (dashed line).

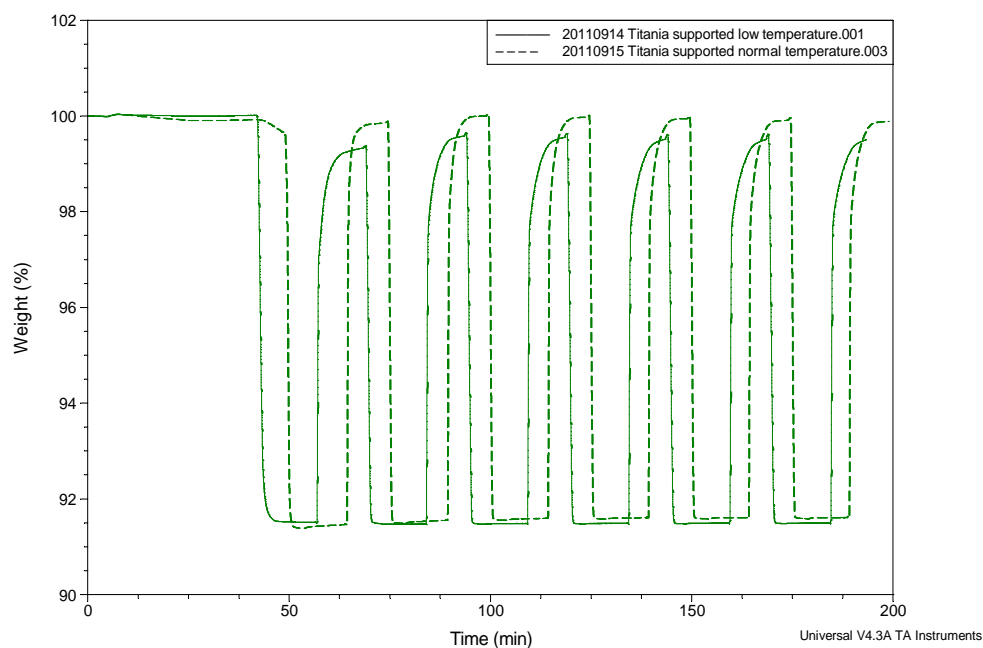


Figure 28. Titanium(IV) oxide as an oxygen carrier support at 650°C and 800°C.

The comparison between titanium(IV) oxide and alumina as a supporting material for an oxygen carrier was shown in Figure 27 and Figure 28. Oxygen carriers supported by titanium(IV) oxide and alumina were, respectively, located different supporting material oxygen carriers in TGA, and ran a reduction-oxidation cycling test at both 650°C and 800°C. In Figure 27 and Figure 28, solid lines represent the oxygen carrier at 650°C, and dashed lines refer to the test at 800°C. When the weight begins to drop, the reduction process begins. The copper based oxygen carrier is not completely reduced until the weight of the sample in the TGA is stable. The oxygen carrier with aluminum oxide support (Figure 27) shows the difference between red-ox cycles operated at 650°C and 800°C. Although the copper(II) oxide loading is the same, the weight loss shows different. At 650°C, the weight loss from reduction is less than that at 800°C. At a lower

temperature, the oxygen carrier supported by titanium(IV) oxide apparently had better performance on reduction conversion factor than supported on alumina.

3.3 Activity Test

3.3.1 Operation Difference

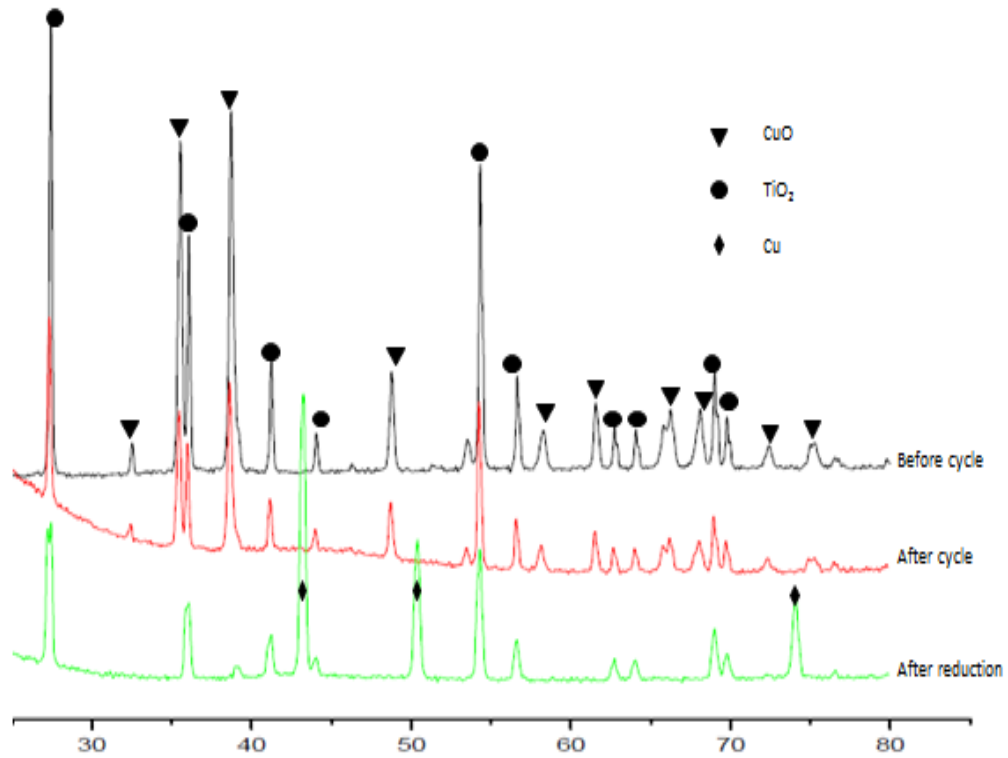


Figure 29. XRD pattern of oxygen carriers before, after cycles and reduced.

To study the activity of copper-based oxygen carriers on titanium(IV) oxide in operation, the samples were subject to running reduction-oxidation cycles. The samples before and after reduction, as well as after 20 red-ox cycles were analyzed by XRD. Their XRD patterns are shown in Figure 29. The initial oxygen carriers were shown as a mixture of copper(II) oxide and titanium(IV) oxide. After reduction reaction, the copper(II) oxide donated oxygen in the fuel reactor. The pattern for the reduced oxygen carrier (bottom curve Figure 29) shows no copper(II) oxide peaks, only copper peaks.

After 20 cycles of reduction and oxidation, the sample's XRD pattern (middle curve of the Figure 29) was very similar. The position of peaks and ratio of intensity were almost the same. During the reduction and oxidation process, the phase and structure of oxygen carrier changed little, which is the precondition of better durability. Due to the effect of sample holder of XRD, the base line of curve after cycles before 2 theta equaled to 30° was not horizontal. This does not affect the ratio of each peak in its curve, but the total intensity will be decreased.

3.3.2 Reactivity

The oxidation activity for the oxygen carriers prepared via different methods was compared using the weight gain plot from the TGA tests. The oxidation time was defined as the time from initial weight gain to the weight until the weight is stable for 30 seconds. According to the derivative weight plot, the oxidation process was divided into two parts, high rate periods (oxidation is fast) and low rate periods (oxidation is slow). High rate period is when oxidation begins up until the onset point. The period from the onset point to the end of the oxidation is considered the low rate period. The rest time to the end of oxidation process was named as low rate period.

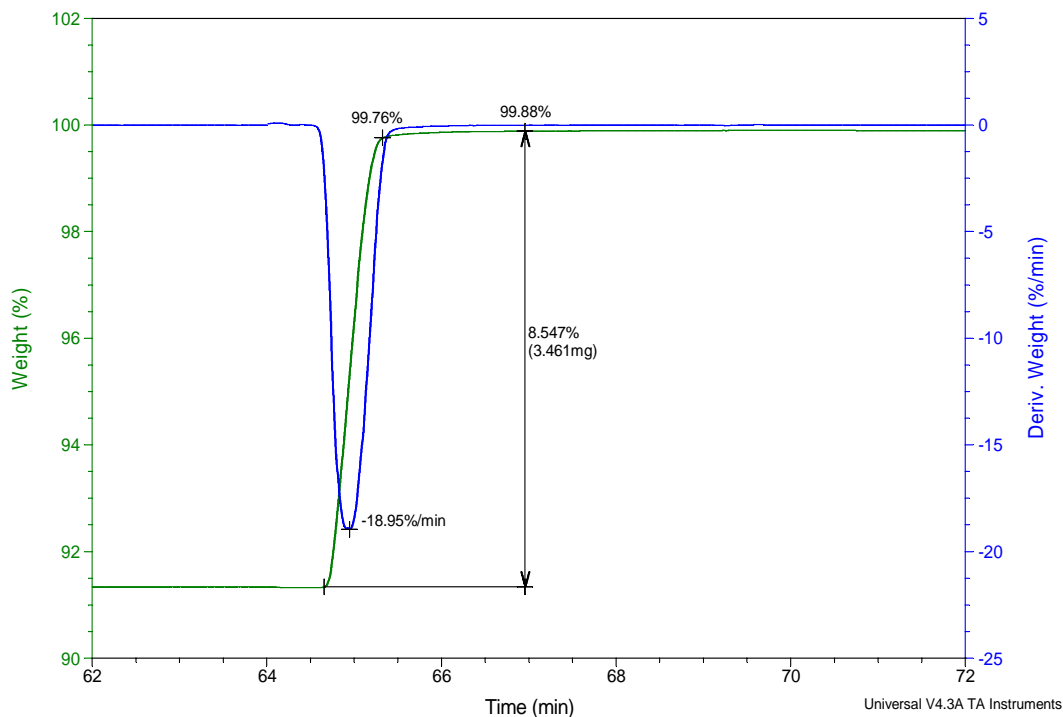


Figure 30. Oxidation process of sol-gel sample.

Figure 30 shows the weight loss profile for the oxygen carrier from sol-gel method operated in TGA at 800°C. The high rate period was 0.63 minutes. At the end of this time, 97.2% of the oxidation process was complete. The remaining oxidation took place in 1.61 minutes. When the reaction rate slowed down, the oxygen carrier used 1.61 minute to finish the oxidation process, reached the conversion of 98.6%. So the total oxidation time for oxygen carrier from sol-gel method was 2.24 minute.

Sample: titanium copper oxide 10min ox
Size: 21.1830 mg
Method: Titanium oxide mehtod

TGA

File: titanium copper oxide longer oxidatio...

Run Date: 19-Aug-2011 08:19
Instrument: 2950 TGA HR V5.4A

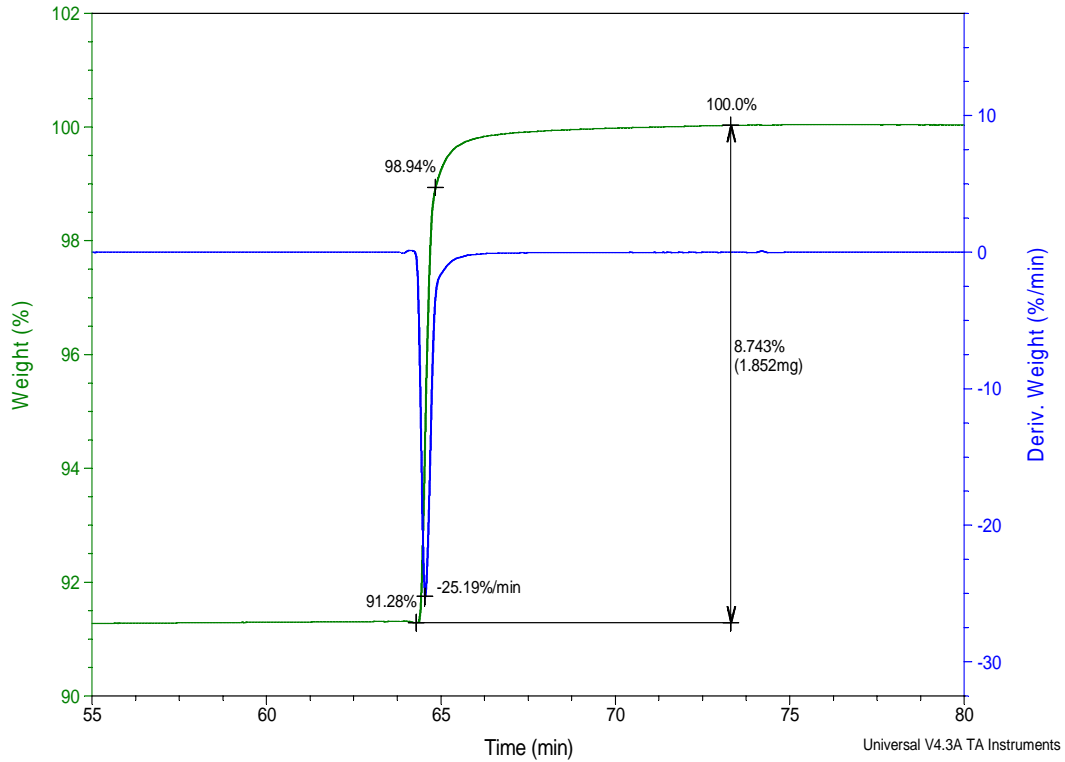


Figure 31. Oxidation process of co-precipitation method.

The oxidation reaction for the co-precipitation prepared oxygen carrier took place in 8.99 minutes with the higher period lasting 0.62 minutes (88.1% complete) and the low rate period 8.37 minutes (100% complete)

Sample: 20120131 wet im cycle3
Size: 65.9100 mg

TGA

File: ...20120131 wet impregnation cycle1.003

Run Date: 01-Feb-2012 10:08
Instrument: 2950 TGA HR V5.4A

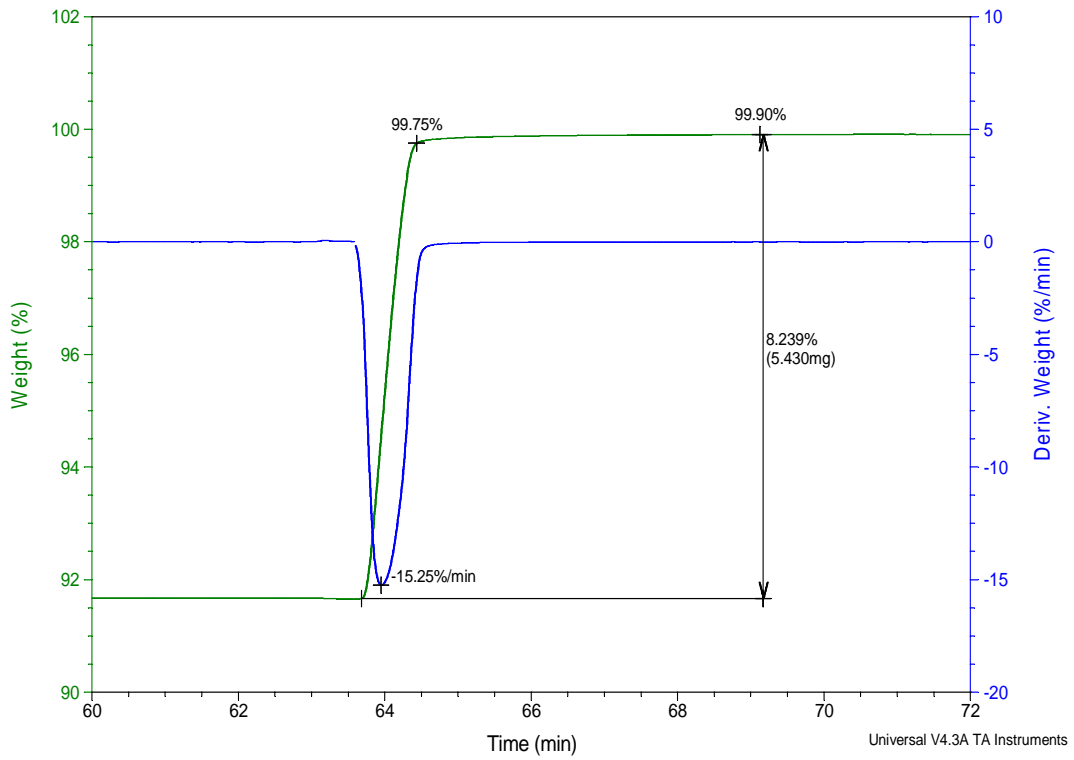


Figure 32. Oxidation process of wet-impregnation sample.

The oxidation reaction for the co-precipitation prepared oxygen carrier took place in 5.50 minutes with the higher period lasting 0.86 minutes (96.7% complete) and the low rate period 4.64 minutes (100% complete)

Sample: 20120201 mech mix cycle
Size: 46.5680 mg

TGA

File: ...20120201 mechanical mixing cycle.004

Run Date: 02-Feb-2012 09:53
Instrument: 2950 TGA HR V5.4A

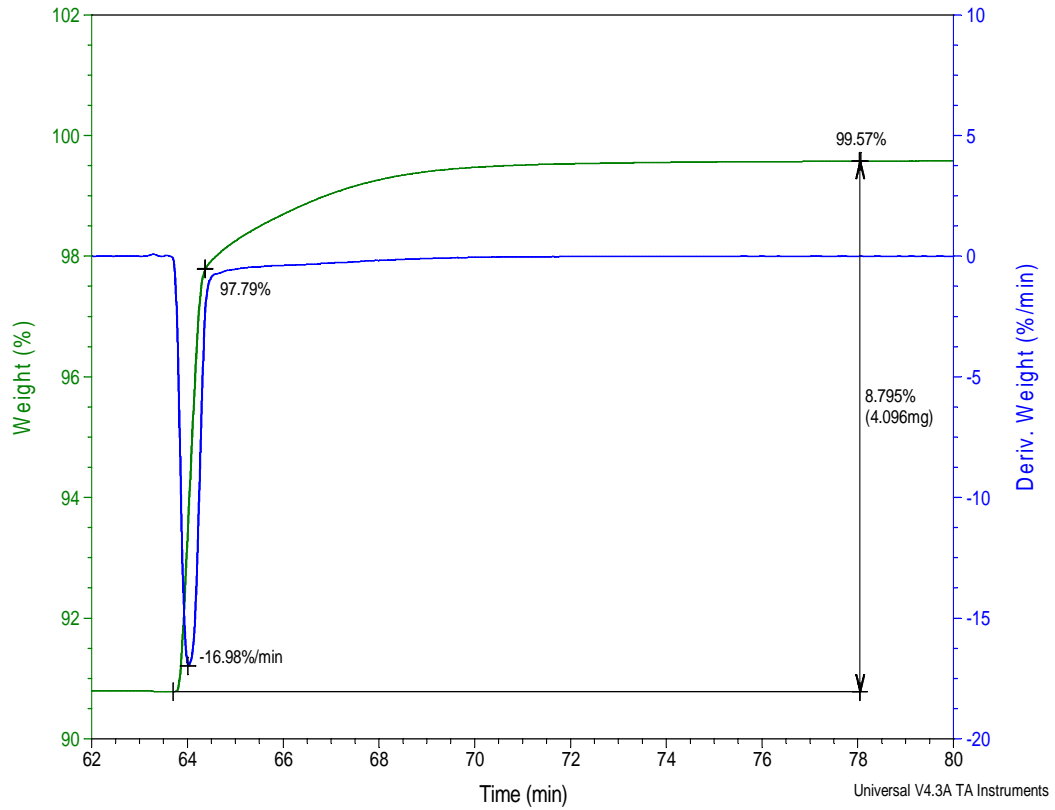


Figure 33. Oxidation process of mechanical mixing sample.

The oxidation reaction for the co-precipitation prepared oxygen carrier took place in 14.29 minutes with the higher period lasting 0.67 minutes (75.9% complete) and the low rate period 13.62 minutes (100% complete)

Table 9. Oxidation comparison between different preparation methods.

Method	Mechanical Mix	Wet- Impregnation	Sol-gel	Co- precipitation
Oxidation time/min	14.29	5.50	2.24	8.99
High rate period	0.67 min to 75.9%	0.86 min to 96.7%	0.63 min to 97.2%	0.62 min to 88.1%
Low rate period	13.6 min 75.9% to 95.1%	4.6 min 96.7% to 98.8%	1.6 min 97.2% to 98.6%	8.4 min 88.1% to 100%

The oxidation activity performance and reaction time of oxygen carriers from different preparation methods are shown in Table 9. Comparing the data from the three plots, oxygen carriers from the sol-gel preparation method experienced less time than other three methods to finish the oxidation process. For the high rate period, the sample from the sol-gel method spent similar time with the other three methods to perform higher conversion. For the low rate period, the sol-gel oxygen carriers required less time to reach the end of the reaction. According to the analysis above, oxygen carriers prepared from the sol-gel method have a better activity rate and a shorter reaction time for oxidation than the wet-impregnation method, the mechanical mixing, and co-precipitation method.

3.3.3 Temperature

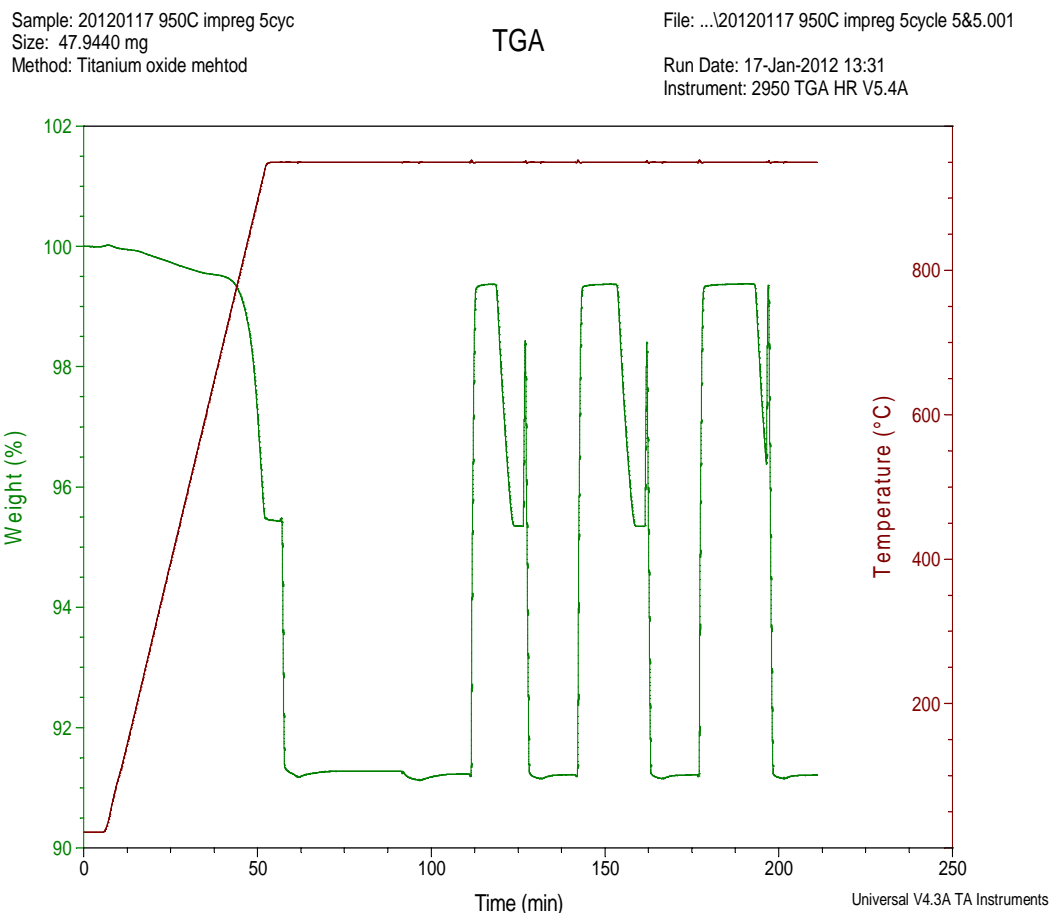


Figure 34. Oxygen carrier with titanium(IV) oxide operated red-ox cycles at 950°C.

The weight loss vs. time plot for the oxygen carrier with titanium(IV) oxide support at 950°C is shown in Figure 34. Due to the decomposition of copper(II) oxide at high temperature, especially in an oxygen poor environment, copper(II) oxide released oxygen and produced copper(I) oxide. The temperature at which copper(II) oxide formed copper(I) oxide depended on the amount of oxygen in the environment. The more oxygen in the environment, the quicker oxygen escapes from copper(II) oxide molecules.

From the weight loss figure 34, before reduced by hydrogen, the decomposition weight loss was just half of the total weight loss of reduction. The weight gain before

reduction was caused by the oxygen from air remaining in the gas inlet. After gas switching, there is still a little amount of air remaining in the pipe.

Degradation

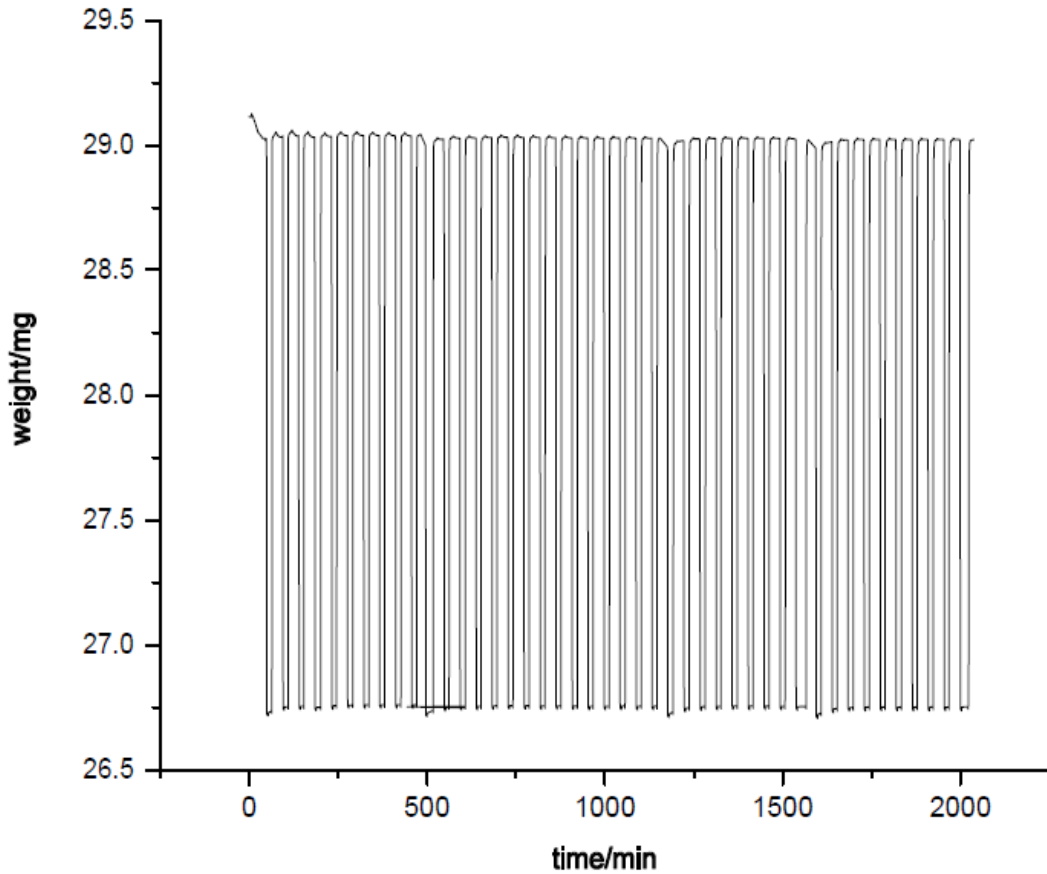


Figure 35. Oxygen carrier with titanium(IV) oxide in 45 red-ox cycles.

Durability is one of the most important factors of an oxygen carrier. After multiple cycles²⁵, the structure between molecules can change. Because of the low melting point, copper tends to agglomerate, even despite the inert support material that disperses the oxygen carrier. The agglomeration will definitely cause some copper or copper(II) oxide inactivity, resulting in degradation. To study degradation, an oxygen carrier prepared using the sol-gel method was subject to multiple red-ox cycles in the TGA. Weight loss indicates a loss or transport of oxygen throughout the process. The

weight loss vs. time plot after 45 cycles is shown in Figure 35. The weight loss profile shows very stable weight loss gain indicating very little degradation.

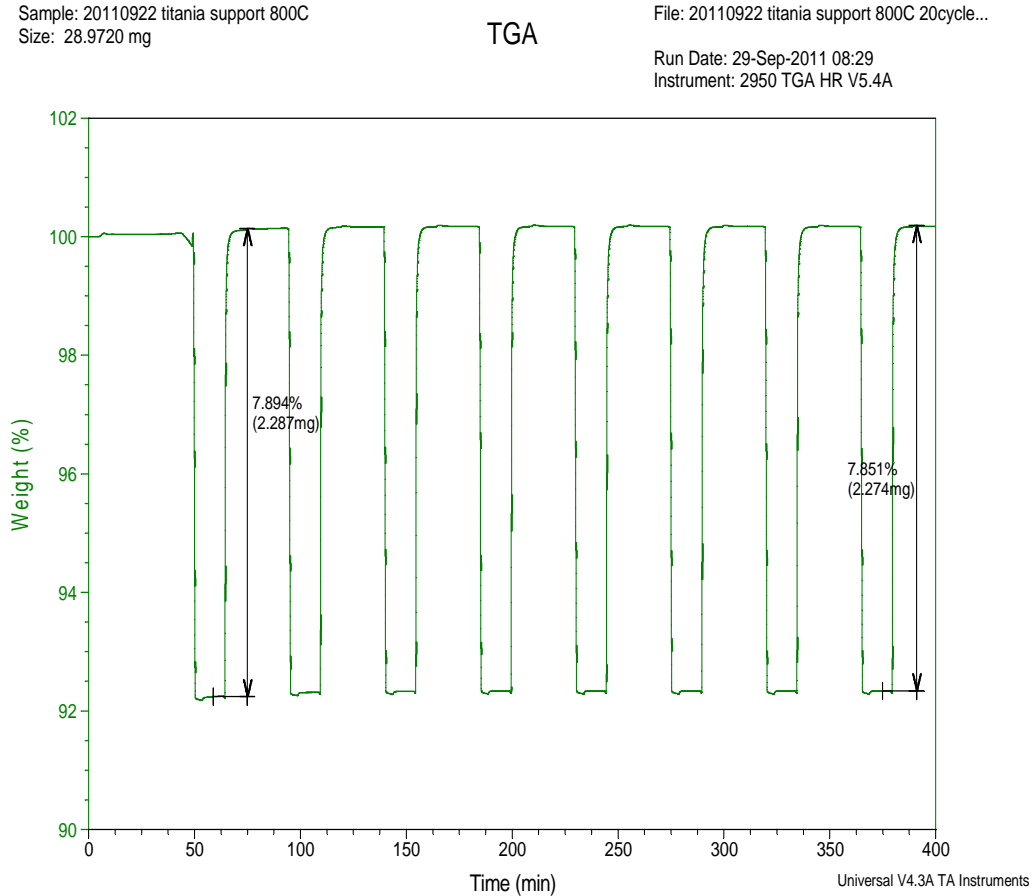


Figure 36. Oxygen carrier with titanium(IV) oxide from sol-gel method operated in 8 red-ox cycles.

Figure 36 shows the oxygen carrier operated for 8 red-ox cycles, which is a part of the previous 45 cycles. According to the data shown in the plot, during 8 cycles, the weight loss changed from 7.89% to 7.85%, which referred to 0.04% oxygen carrying ability degradation. This performance would be quite acceptable in future industrial applications.

Kinetics

In figure 37, oxidation reaction of copper-based oxygen carrier on titanium(IV) oxide prepared from sol-gel method, was transferred to the Hancock and Sharp plots from weight vs. time plot.

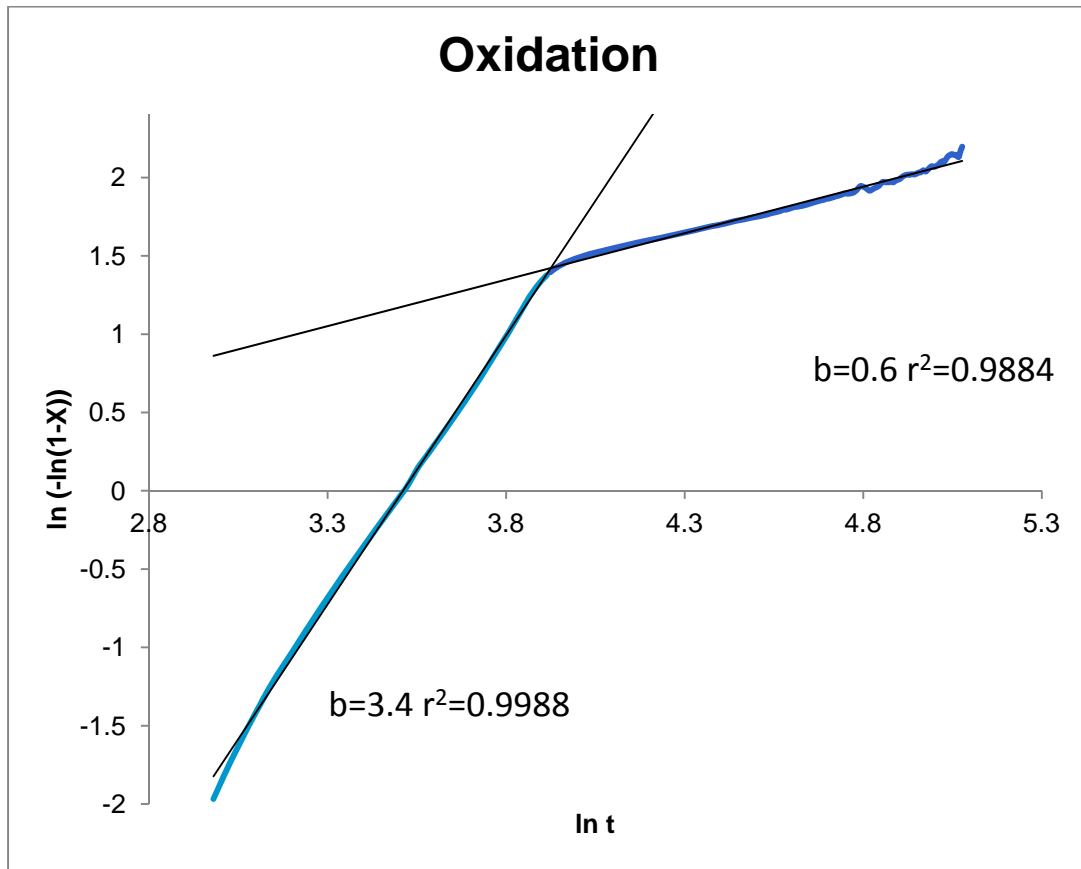


Figure 37. Oxidation kinetics.

As shown in Figure 37, the oxidation process can be separated into two periods, the nucleation model and the diffusion model. The two models simply describe the high rate and low rate periods. Therefore, the oxidation process can be described according to the two models. When the oxygen in the air connects with the surface of the oxygen carrier, copper(II) oxide is produced. At the beginning of the reaction, most of the oxygen carrier surface area is available, resulting in a fast oxidation reaction. As the surface

becomes covered by reaction products, the reaction slows down and only the inner parts of the carrier can react at oxygen as it diffuses resulting in a slower reaction rate.

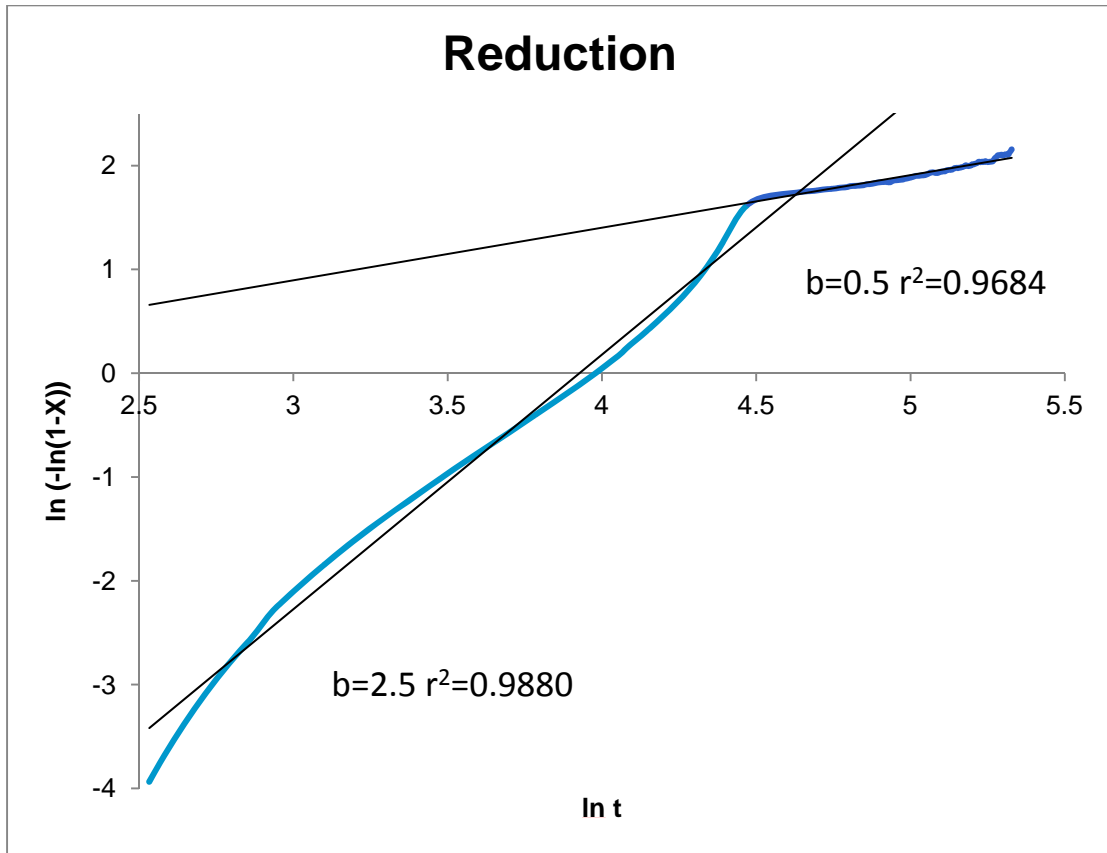


Figure 38. Reduction kinetics.

According to the plot shown in Figure 38, the reduction process is similar to the oxidation process in that it can be divided into two periods, nucleation reaction and diffusion controlled period. The result also can be well matched with the activity test result.

4. Conclusion

In this study, copper-based oxygen carriers on titanium(IV) oxide supports were prepared and characterized. The interaction between copper(II) oxide and titanium(IV) oxide was investigated from the XRD pattern of the oxygen carrier calcinated at different temperatures. Copper cannot combine with titanium(IV) oxide to produce copper(II) titanate until a very high temperature (over 1000°C); at that temperature, copper(II) oxide melted due to a low melting point.

The reduction activity of oxygen carriers on titanium(IV) oxide supports were compared with alumina supports. As an inert binder, the titanium(IV) oxide supported oxygen carrier had a better activity for reduction process at 650°C than the oxygen carrier supported by alumina. For the sample supported by titanium(IV) oxide, the reduction curve at 650°C was the same as the sample at 800°C. However, with alumina sample, the conversion of reduction process was no more than 90%.

In this study, besides the sol-gel method, three other methods were used to synthesis oxygen carriers: mechanical mixing, wet-impregnation and co-precipitation method. When comparing these four methods, the sol-gel method had better performance in many respects. Copper(II) oxide dispersions of the oxygen carrier from these preparation methods were compared through variance of copper(II) oxide ratio of each sample. The variance of the sol-gel method was less than those of the other three methods. Moreover, the oxidation activity of the sol-gel sample was better than all of the other preparation methods utilized in this study. For the oxidation process, sol-gel oxygen carriers also had the shortest reaction time in the four methods. Therefore, sol-gel method is a better candidate for synthesizing oxygen carriers than other methods.

The oxygen carriers from the sol-gel method were set in multiple red-ox cycles to test degradation. After 45 red-ox cycles, the degradation was only 8%. The XRD patterns of initial oxygen carriers, the carrier after reduction, and the carrier after a 20-cycle reduction-oxidation cycle were investigated. The carrier after reduction indicated no copper(II) oxide peaks existence. During the reduction process, copper based oxygen carriers showed high activity. The pattern after 45 cycles had the same peak positions and ratios with the initial carrier pattern. After 45 cycles, the phase and structure of the oxygen carrier particles changed very little. Therefore, the oxygen carriers, synthesized by the sol-gel method had good stability.

There were two different predominant Kinetics of oxygen carriers' reaction process: nucleation period and diffusion period. At the very beginning of the reaction, copper or copper(II) oxide as product for oxidation or reduction, respectively, was generated at the surface of the particle. These product as nuclear at the surface of particles grew up very fast due to being easily connected with reactive gas. When the particle surface was covered by product, diffusion controlled the rate of the reactions, which slowed down the reaction rate.

5. Future Work

In this study, all the TGA activity tests used hydrogen as a reducing agent. In industry, oxygen carriers would be reduced by fuel, such as carbon monoxide, methane, or other gaseous fuel. Those compounds are more complex than hydrogen. Carbon deposits should be a factor when evaluating an oxygen carrier. The reducibility of fuel should be much lower than hydrogen. So future work, should focus on the activity of carriers in a methane air alternative environment.

Study the process of sol-gel preparation method; examine different factors, such as gelation temperature, ripening time and temperature. Study the reaction at the microscopic scale including the structural change and the resulting activity effect.

BIBLIOGRAPHY

1. National Aeronautics and Space Administration (NASA)
<http://climate.nasa.gov/keyIndicators/index.cfm#globalTemp> (Accessed Feb 22, 2012)
2. D. S. Jenkinson^{*}, D. E. Adams & A. Wild, Model estimates of CO₂ emissions from soil in response to global warming, *Nature* **351**, 304 – 306
3. Daniel A. Lashof, The dynamic greenhouse: Feedback processes that may influence future concentrations of atmospheric trace gases and climatic change, *Climate Change*, **1989**, 14, 213-242
4. National Aeronautics and Space Administration (NASA)
<http://climate.nasa.gov/evidence/> (Accessed Feb 22, 2012)
5. U.S. Energy Information Administration
6. http://www.eia.doe.gov/cneaf/electricity/epm/Table1_1.html (Accessed Feb 06, 2011)
7. Hongqun Yang, Zhenghe Xu, Maohong Fan, Rajender Gupta, Rachid B Slimane, Alan E Bland, Ian Wright, Progress in Carbon Dioxide Separation and Capture: A Review, *Journal of Environmental Sciences*, **2008**, 14-27
8. Feron P H M, Hendriks C A, CO₂ Capture Process Principles and Costs, *Oil and Gas Science and Technology Rev*, **2005**, 60(3): 451-459
9. J. Ada'nez,^{*} L. F. de Diego, F. Garcí'a-Labiano, P. Gaya'n, and A. Abad, Selection of Oxygen Carriers for Chemical-Looping Combustion, *Energy & Fuels*, **2004**, 18, 371-377
10. Yan Cao, Wei-Ping Pan, Investigation of Chemical Looping Combustion by Solid Fuels. 1.Process Analysis, *Energy & Fuels* **2006**, 20, 1836-1844

11. Villa, R., Cristiani, C., Groppi, G., Lietti, L., Forzatti, P., Cornaro, U., Rossini, S., Ni Based Mixed Oxide Materials for CH₄ Oxidation Under Redox Cycle Conditions, *Journal of Molecular Catalysis A: Chemical*, **2003**, 204–205, 637–646
12. Cao, Y.; Casenas, B.; Pan, W. P. Investigation of Chemical Looping Combustion by Solid Fuels. 2. Redox Reaction Kinetics and Product Characterization with Coal, Biomass, and Solid Waste as Solid Fuels and CuO as an Oxygen Carrier. *Energy Fuels* **2006**, 20 (5), 1845–1854
13. J. A. Wang, X. Bokhimi, A. Morales, and O. Novaro, T. Lo'pez and R. Go'mez, Aluminum local environment and defects in the crystalline structure of sol-gel alumina catalyst, *J. Phys. Chem. B*, **1999**, 103, 299-303
14. Toxicology and Carcinogenesis Studies of Nickel Oxide, *U.S. Dept. of Health and Human Services*, **1996**, 07, 451
15. Abad, A., Adanez, J., Garcia-Labiano, F., de Diego, L., Gayan, P., Celaya, J., Mapping of the range of operational conditions for Cu-, Fe-, and Ni-based oxygen carriers in chemical-looping combustion, *Chemical Engineering Science*, **2007**, 62, 533-549
16. Cho, P., Mattisson, T., Lyngfelt, A., Defluidization conditions for a fluidized bed of iron oxide-, nickel oxide-, and manganese oxide-containing oxygen carriers for chemical-looping combustion, *Industrial & Engineering Chemistry Research*, **2006**, 45, 968–977
17. De Diego, L. F.; Garcia-Labiano, F.; Adanez, J.; Gayan, P.; Abad, A.; Corbella, B. M.; Palacios, J. M. Development of Cu-based oxygen carriers for chemical-looping combustion. *Fuel* **2004**, 83 (13), 1749–1757

18. Corbella, B.M., de Diego, L.F., Gracia-Labiano, F., Adanez, J., Palacios, J.M., Characterization study and five-cycle tests in a fixed-bed reactor of titania supported nickel oxide as oxygen carriers for the chemical-looping combustion of methane., *Environmental Science & Technology*, **2005**, 39, 5736–5803
19. Johansson, M.; Mattisson, T.; Lyngfelt, A. Creating a Synergy Effect by Using Mixed Oxides of Iron and Nickel Oxides in the Combustion of Methane in a Chemical-Looping Combustion Reactor. *Energy Fuels* **2006**, 20 (6), 2399–2407
20. J. Adanez, L. F. de Diego, F. Garcia-Labiano, P. Gaya'n, and A. Abad, Selection of oxygen carriers for chemical-looping combustion, *Energy & Fuels*, **2006**, 20, 1836-1844
21. Hancock, J. D.; Sharp, J. H. Method of Comparing Solid-State Kinetic Data and Its Application to the Decomposition of Kaolinite, Brucite, and BaCO₃. *J. Am. Ceram. Soc.* **1972**, 55, 74–77
22. Sung Real Son, Kang Seok Go, and Sang Done Kim, Thermogravimetric Analysis of Copper(II) Oxide for Chemical-Looping Hydrogen Generation, *Ind. Eng. Chem. Res.* **2009**, 48, 380–387
23. Vidya Joshi, Kenneth R. Morris, Stephen R. Byrn, and M. Teresa Carvajal, Evaluation of the Use of E_a (Activation Energy) as a Quantitative Indicator of Physical Stability of Indomethacin Solvates: Methanolate and Tertiary Butyl Alcohol Solvate, *Crystal Growth & Design*, **2009**, Vol. 9, 3359-3366
24. Piotrowski, K.; Mondal, K.; Lorethova, H.; Stonawski, L.; Szymanski, T.; Wiltowski, T. Effect of Gas Composition on the Kinetics of Iron Oxide Reduction in a Hydrogen Production Process. *Int. J. Hydrogen Energy* **2005**, 30, 1543–1554

25. Piotrowski, K.; Mondal, K.; Wiltowski, T.; Dydo, P.; Rizeg, G. Topochemical Approach of Kinetics of the Reduction of Hematite to Wüstite. *Chem. Eng. J.* **2007**, *131*, 73–82
26. B. M. Corbella, L. De Diego, F. Garcí'a, J. Ada'nez, and J. M. Palacios, The Performance in a Fixed Bed Reactor of Copper(II)-Based Oxides on Titania as Oxygen Carriers for Chemical Looping Combustion of Methane, *Energy & Fuels* **2005**, *19*, 433-441
27. James A. Schwarz, Methods for preparation of catalytic materials, *Chem. Rev.* **1995**, *95*, 477-510
28. S. J Teichner, *Chem. Technol.* **1991**, *21*, 372
29. Haibo Zhao, Liming Liu, Baowen Wang, Di Xu, Linlin Jiang, and Chuguang Zheng, Sol–Gel-Derived NiO/NiAl₂O₄ Oxygen Carriers for Chemical-Looping Combustion by Coal Char, *Energy & Fuels*, **2008**, *22*, 898–905
30. Chen-Chi Wang and Jackie Y. Ying, Sol-Gel Synthesis and Hydrothermal Processing of Anatase and Rutile Titania Nanocrystals, *Chem. Mater.* **1999**, *11*, 3113-3120
31. Patnaik, P. *Dean's Analytical Chemistry Handbook*, 2nd ed. McGraw-Hill, **2004**
32. Jin, H. G.; Hong, H.; Wang, B. Q.; Han, W.; Lin, R. M. A new principle of synthetic cascade utilization of chemical energy and physical energy. *Sci. China Ser. E-Eng. Mater. Sci.*, **2005**, *48* (2), 163–179

ACTIVITIES

Presentation:

1. Yaowen Cui, Yan Cao, Wei-Ping Pan, Preparation of copper-based oxygen carrier supported on titanium(IV) oxide, 243rd American Chemistry Society Annual Meeting, 2012, March
2. Yaowen Cui, Yin Liu, Yan Cao, Wei-Ping Pan, Preparation of copper-based oxygen carrier using coprecipitation method , The 96th Kentucky Academic Science Annual Meeting, Western Kentucky University, Bowling Green, KY, November 13. 2010
3. Yaowen Cui, Yan Cao, Wei-Ping Pan, Preparation of copper-based oxygen carrier supported on titanium(IV) oxide, The 97th Kentucky Academy of Science Annual Meeting, Murray State University, Murray, KY, November 04. 2011 (**2011 Graduate**

Research Competition Awards)

4. Yaowen Cui, Yan Cao, Wei-Ping Pan, Preparation of copper-based oxygen carrier with co-precipitation and granulation method, The 41st Annual WKU Student Research Conference, March 26, 2012
5. Yaowen Cui, Yan Cao, Wei-Ping Pan, Preparation of copper-based oxygen carrier supported on titanium(IV) oxide, The 42nd Annual WKU Student Research Conference, March 24, 2012

Publication:

1. Yaowen Cui, Yan Cao, Wei-Ping Pan, Preparation of copper-based oxygen carrier supported on titanium(IV) oxide, Preprints of symposia-American Chemical Society, Fuel Chemistry, 2012

2. Yaowen Cui, Yan Cao, Wei-Ping Pan, Preparation of copper-based oxygen carrier supported on titanium(IV) oxide. (Paper for submission)

